

# Reversible O–H bond activation by tripodal tris(nitroxide) aluminum and gallium complexes.

*Joseph S. Scott,<sup>1</sup> Mika L. Maenaga,<sup>1</sup> Audra J. Woodside,<sup>1</sup> Vivian W. Guo,<sup>1</sup> Alex R. Cheriell,<sup>1</sup> Michael R. Gau,<sup>2</sup> Paul R. Rablen,<sup>1</sup> Christopher R. Graves<sup>1,\*</sup>*

<sup>1</sup> Department of Chemistry & Biochemistry, Swarthmore College, 500 College Avenue, Swarthmore, PA 19081, United States

<sup>2</sup> Department of Chemistry, University of Pennsylvania, 231 South 34<sup>th</sup> Street, Philadelphia, PA 19104, United States

## Electronic Supplementary Information

Author contribution statement	S3
<b>Figure S1.</b> <sup>1</sup> H NMR spectrum of (TriNOx <sup>3-</sup> )Al ( <b>1</b> )	S4
<b>Figure S2.</b> <sup>13</sup> C{ <sup>1</sup> H} spectrum of (TriNOx <sup>3-</sup> )Al ( <b>1</b> )	S5
<b>Figure S3.</b> <sup>1</sup> H NMR spectrum of (TriNOx <sup>3-</sup> )Ga ( <b>2</b> )	S6
<b>Figure S4.</b> <sup>13</sup> C{ <sup>1</sup> H} NMR spectrum of (TriNOx <sup>3-</sup> )Ga ( <b>2</b> )	S7
<b>Figure S5.</b> <sup>1</sup> H NMR spectrum of (TriNOx <sup>3-</sup> )In ( <b>3</b> )	S8
<b>Figure S6.</b> <sup>13</sup> C{ <sup>1</sup> H} NMR spectrum of (TriNOx <sup>3-</sup> )In ( <b>3</b> )	S9
<b>Figure S7.</b> <sup>1</sup> H NMR spectrum of (HTriNOx <sup>2-</sup> )Al–O'Bu ( <b>4</b> )	S10
<b>Figure S8.</b> <sup>13</sup> C{ <sup>1</sup> H} NMR spectrum of (HTriNOx <sup>2-</sup> )Al–O'Bu ( <b>4</b> )	S11
<b>Figure S9.</b> <sup>1</sup> H NMR spectrum of (HTriNOx <sup>2-</sup> )Al–OBn ( <b>6</b> )	S12
<b>Figure S10.</b> <sup>13</sup> C{ <sup>1</sup> H} NMR spectrum of (HTriNOx <sup>2-</sup> )Al–OBn ( <b>6</b> )	S13
<b>Figure S11.</b> <sup>1</sup> H NMR spectrum of (HTriNOx <sup>2-</sup> )Al–OPh ( <b>8</b> )	S14
<b>Figure S12.</b> <sup>13</sup> C{ <sup>1</sup> H} NMR spectrum of (HTriNOx <sup>2-</sup> )Al–OPh ( <b>8</b> )	S15
<b>Figure S13.</b> <sup>1</sup> H NMR spectrum of (HTriNOx <sup>2-</sup> )Ga–OPh ( <b>9</b> )	S16
<b>Figure S14.</b> <sup>13</sup> C{ <sup>1</sup> H} NMR spectrum of (HTriNOx <sup>2-</sup> )Ga–OPh ( <b>9</b> )	S17
Protocol for determination of Lewis acid acceptor numbers for <b>1</b> and <b>2</b>	S18

<b>Figure S15.</b> Stacked plot of the $^{31}\text{P}\{^1\text{H}\}$ NMR spectra of the mixtures of $\text{Et}_3\text{PO}$ (i) and $\text{Et}_3\text{PS}$ (ii) experiments run to evaluate the Lewis acidity of complexes <b>1</b> and <b>2</b> .	S18
Protocol for the VT-NMR studies of complexes <b>4</b> , <b>6</b> , and <b>8</b>	S19
<b>Figure S16.</b> Diastereotopic proton region of the $^1\text{H}$ NMR spectra of the <b>4</b> , <b>6</b> , and <b>8</b> complexes over the temperature range 293–353 K.	S19
Protocol for the van't Hoff experiment of <b>1</b> + <i>t</i> -BuOH.	S20
Protocol for determining the $K_{eq}$ values for the reactions of <b>1</b> and <b>2</b> with various alcohols	S20
<b>Figure S17.</b> $^1\text{H}$ NMR spectrum of a 1:1 mixture of <b>1</b> : <i>t</i> -BuOH in $\text{C}_6\text{D}_6$	S21
<b>Figure S18.</b> $^1\text{H}$ NMR spectrum of a 1:1 mixture of <b>1</b> : <i>t</i> -BuOH in $\text{CDCl}_3$	S22
<b>Figure S19.</b> $^1\text{H}$ NMR spectrum of a 1:1 mixture of <b>1</b> : <i>i</i> -PrOH.	S23
<b>Figure S20.</b> $^1\text{H}$ NMR spectrum of a 1:1 mixture of <b>1</b> :9-fluorenemethanol.	S24
<b>Figure S21.</b> $^1\text{H}$ NMR spectrum of a 1:1 mixture of <b>2</b> : <i>t</i> -BuOH in $\text{C}_6\text{D}_6$	S25
<b>Figure S22.</b> $^1\text{H}$ NMR spectrum of a 1:1 mixture of <b>2</b> : <i>t</i> -BuOH in $\text{CDCl}_3$	S26
<b>Figure S23.</b> $^1\text{H}$ NMR spectrum of a 1:1 mixture of <b>2</b> : <i>i</i> -PrOH	S27
<b>Figure S24.</b> $^1\text{H}$ NMR spectrum of a 1:1 mixture of <b>2</b> :1-adamantanol.	S28
<b>Figure S25.</b> $^1\text{H}$ NMR spectrum of a 1:1 mixture of <b>2</b> :BnOH.	S29
<b>Figure S26.</b> $^1\text{H}$ NMR spectrum of a 1:1 mixture of <b>2</b> :9-fluorenemethanol.	S30
<b>Figure S27.</b> $^1\text{H}$ NMR spectrum of a 1:1 mixture of <b>2</b> :propargyl alcohol.	S31
<b>Figure S28.</b> $^1\text{H}$ NMR spectrum of a 1:1 mixture of <b>2</b> : $\text{CF}_3\text{CH}_2\text{OH}$ .	S32
<b>Figure S29.</b> $^1\text{H}$ NMR spectrum of a 1:1 mixture of <b>2</b> : $\text{CCl}_3\text{CH}_2\text{OH}$ .	S33
<b>Figure S30.</b> $^1\text{H}$ NMR spectra of the reaction of <i>t</i> -BuSH with <b>1</b> and <b>2</b>	S34
Protocol for kinetic analysis of the reactions of <b>1</b> and <b>2</b> with alcohols	S35
<b>Figure S31.</b> Plot showing the concentration of products over time for the reaction of <b>1</b> and <b>2</b> with <i>i</i> -PrOH	S35
<b>Figure S32.</b> Initial rate data for the reaction of <b>2</b> with <i>i</i> -PrOH.	S35
Procedure for the calculations to give the predicted- $\text{p}K_a$ of alcohols in DMSO.	S36
<b>Table S1.</b> Raw calculated Gibbs standard free energies at 298 K of alcohols and their corresponding alkoxides.	S37
<b>Table S2.</b> Calculated standard Gibbs free energies of deprotonation ( $\Delta G_{\text{deprot}}$ ) in DMSO for alcohols and the manipulation of that data to give predicted $\text{p}K_a$ values for alcohols.	S38

**Figure S33.** Correlation plot between the G4-calculated versus experimental determined  $pK_a$  values for alcohols. S39

Procedure for the calculations to determine the A-values for the alcohol R groups. S40

**Table S3.** Calculated standard Gibbs free energies at 298 K of the equatorial ( $\Delta G^0_{\text{equatorial}}$ ) and axial ( $\Delta G^0_{\text{axial}}$ ) conformers of R-substituted cyclohexanes and the calculated A-values for the R groups. S40

**Figure S34.** Plot of the  $pK_{eq}$  of the reaction of **2** with alcohol versus the A-value of the alcohol R group. S41

**Author contribution statement.** J.S.S. contributed to the synthesis of **1** and **2** and carried out the Gutmann-Beckett experiments; carried out the reactivity studies between **1** and **2** with alcohols; developed the syntheses and contributed to the characterization of **4**, **6**, **8** and **9**, including all VT-NMR experiments; carried out all  $K_{eq}$  and kinetic experiments; conducted calculations to determine alcohol  $pK_a$  values and R group A-values; drafted and revised the manuscript. M.L.M. contributed to the synthesis of **1** and **2**; carried out preliminary reactivity studies of **1** and **2** with alcohols; contributed to the synthesis and characterization of **4**, **8**, and **9**; contributed to the calculations to determine alcohol  $pK_a$  values; proposed mechanistic considerations. A.J.W. contributed to the synthesis of **1-3**; carried out preliminary reactivity studies of **1** and **2** with alcohols. V. W. G. contributed to the synthesis of **1** and **2**; contributed to the synthesis and characterization of **4**, **6**, **8** and **9**. A.R.C. contributed to the synthesis of **1** and **2**; helped in the drafting and revising of the manuscript. M. R. G. conducted x-ray crystallography. P. R. R. supervised the calculations to determine alcohol  $pK_a$  values and R group A-values. C.R.G. supervised and administered all aspects of the project and drafted and revised the manuscript.

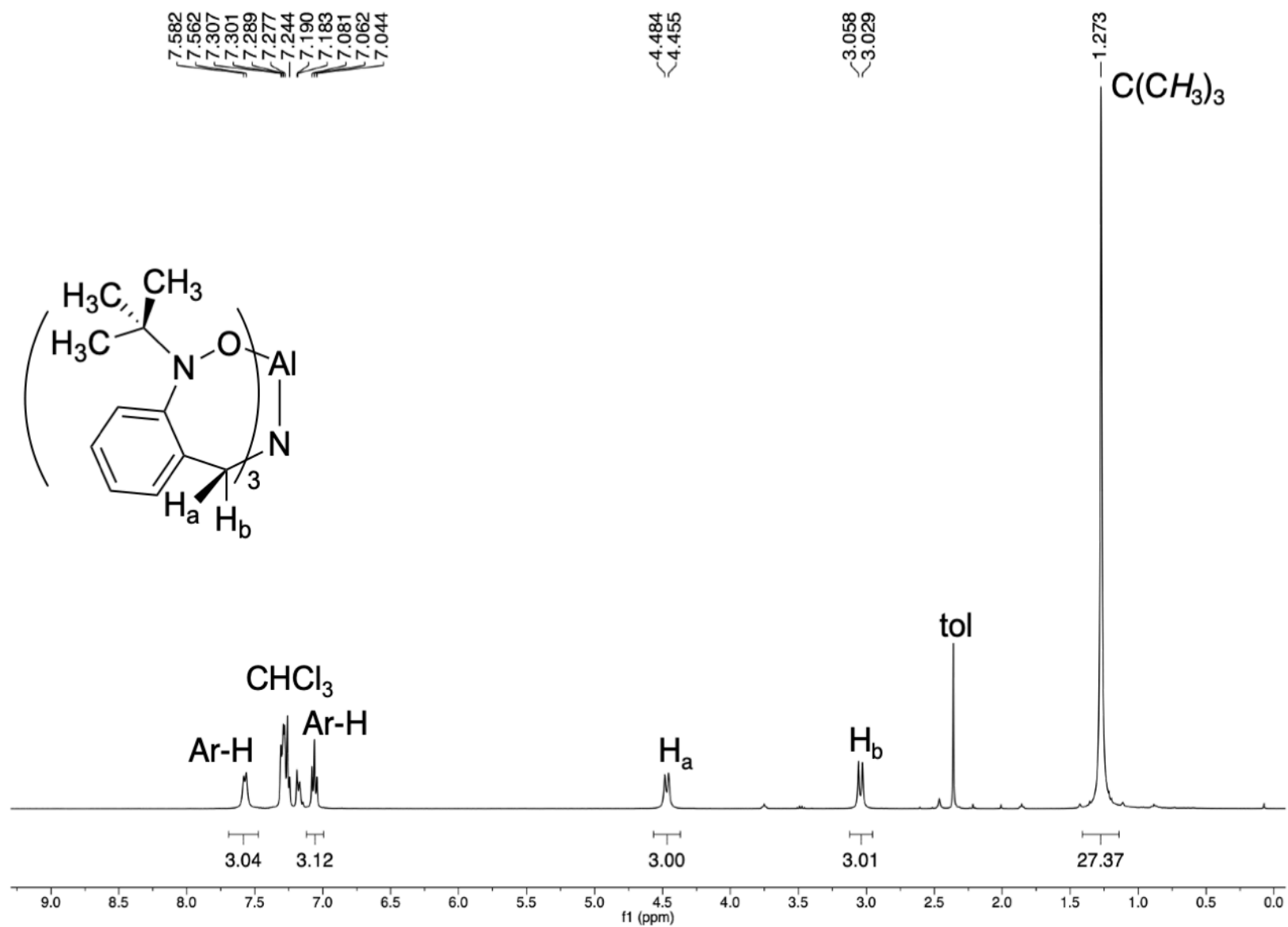


**Figure S1.**  $^1\text{H}$  NMR spectrum of  $(\text{TriNOx}^3)\text{Al}$  (**1**) in  $\text{CDCl}_3$ .

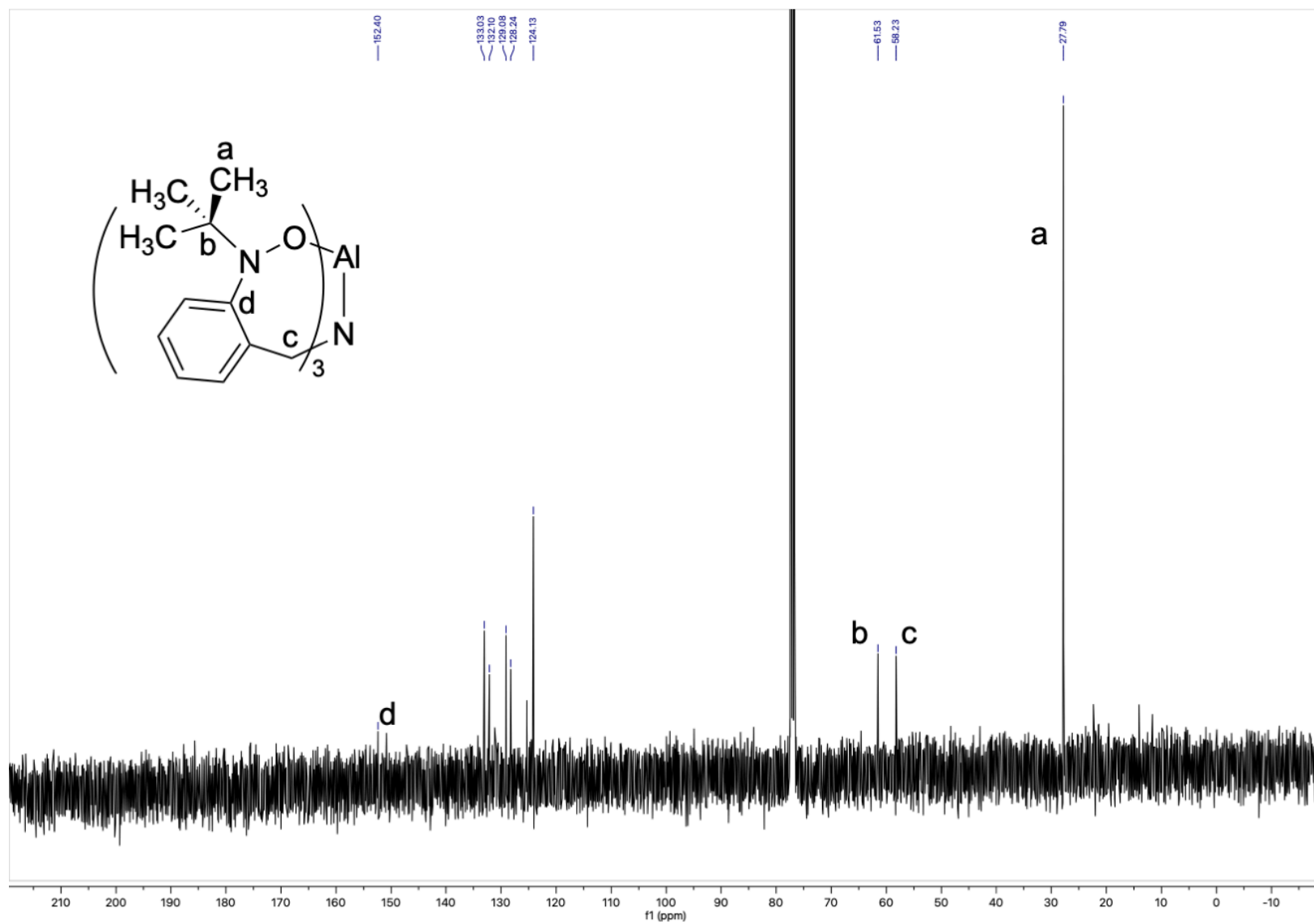


**Figure S2.**  $^{13}\text{C}\{^1\text{H}\}$  NMR spectrum of  $(\text{TriNOx}^{3-})\text{Al}$  (**1**) in  $\text{CDCl}_3$ .

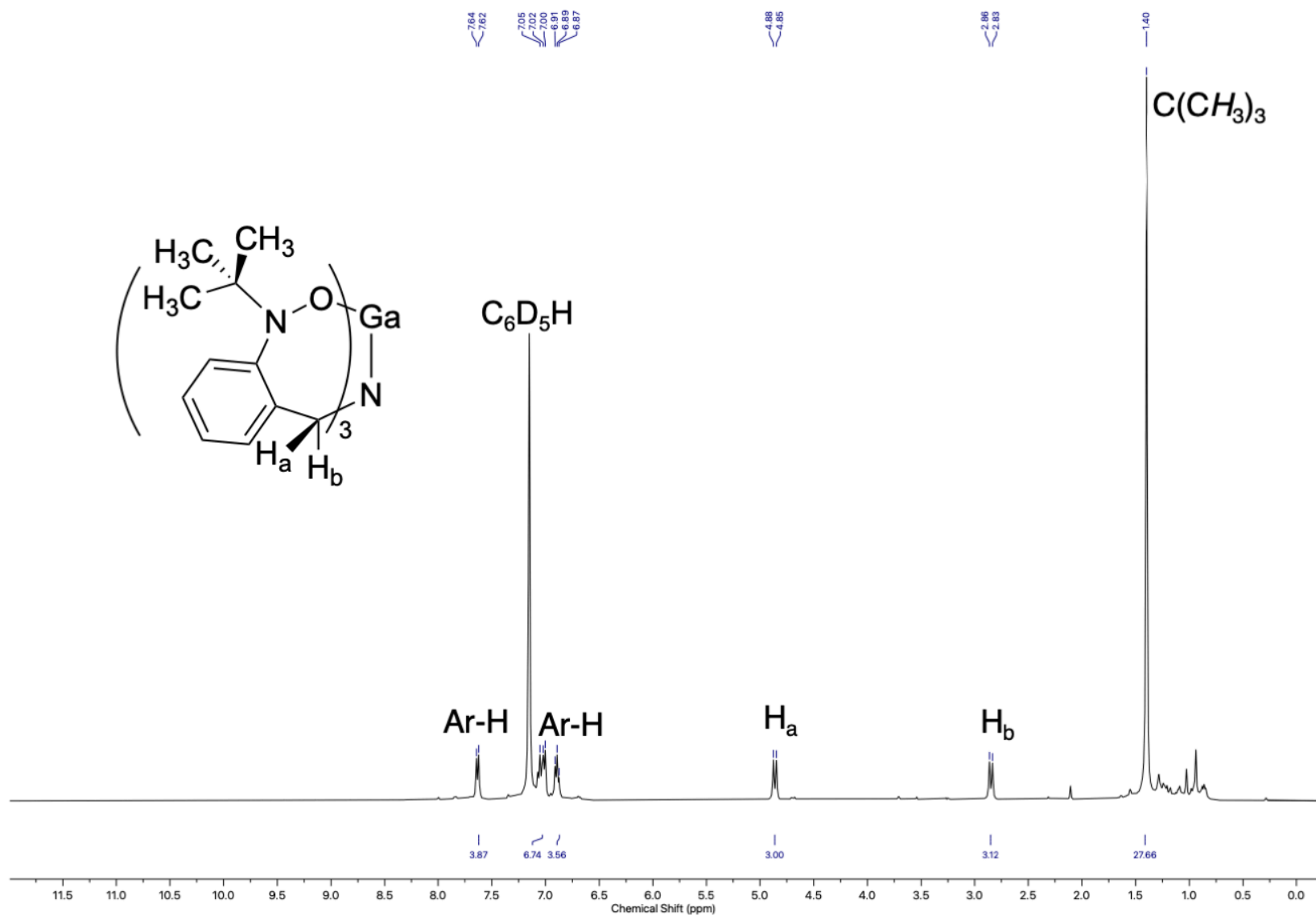


**Figure S3.**  $^1\text{H}$  NMR spectrum of  $(\text{TriNOx}^3)\text{Ga}$  (**2**) in  $\text{C}_6\text{D}_6$ .

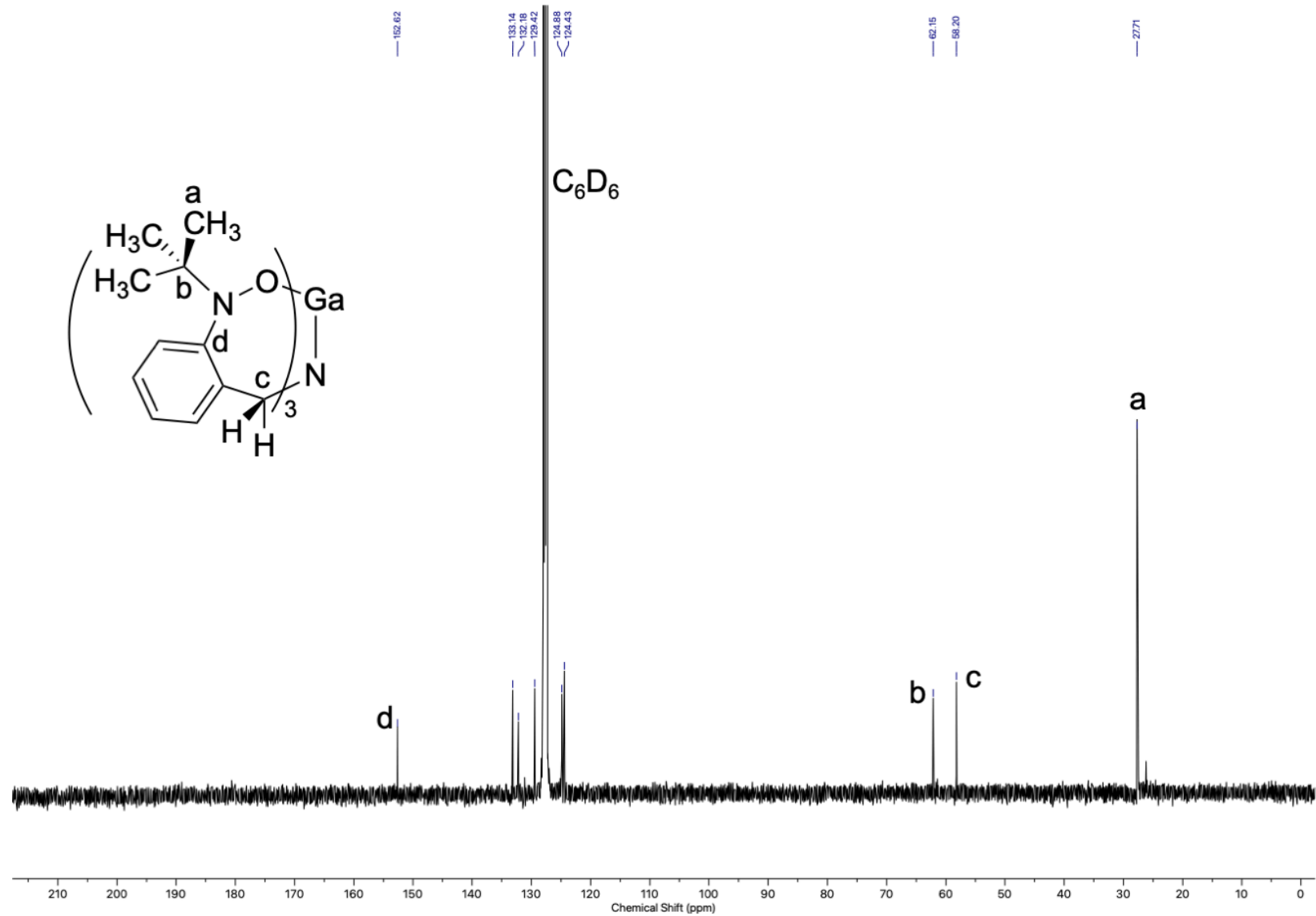


**Figure S4.**  $^{13}\text{C}\{^1\text{H}\}$  NMR spectrum of  $(\text{TriNOx}^3-)\text{Ga}$  (**2**) in  $\text{C}_6\text{D}_6$ .

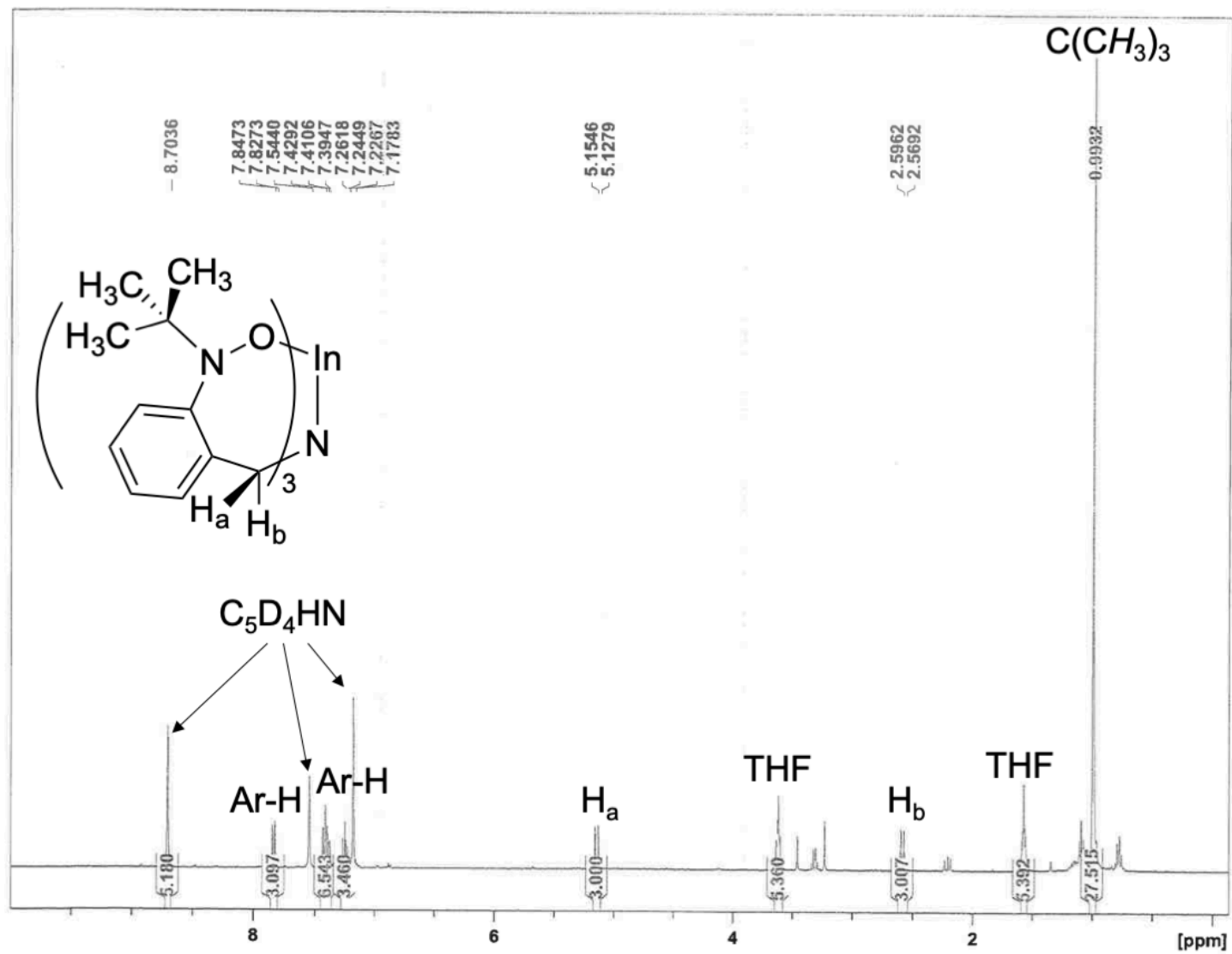


**Figure S5.**  $^1\text{H}$  NMR spectrum of  $(\text{TriNOx}^3-)\text{In}$  (**3**) in  $\text{pyridine-}d_5$ .



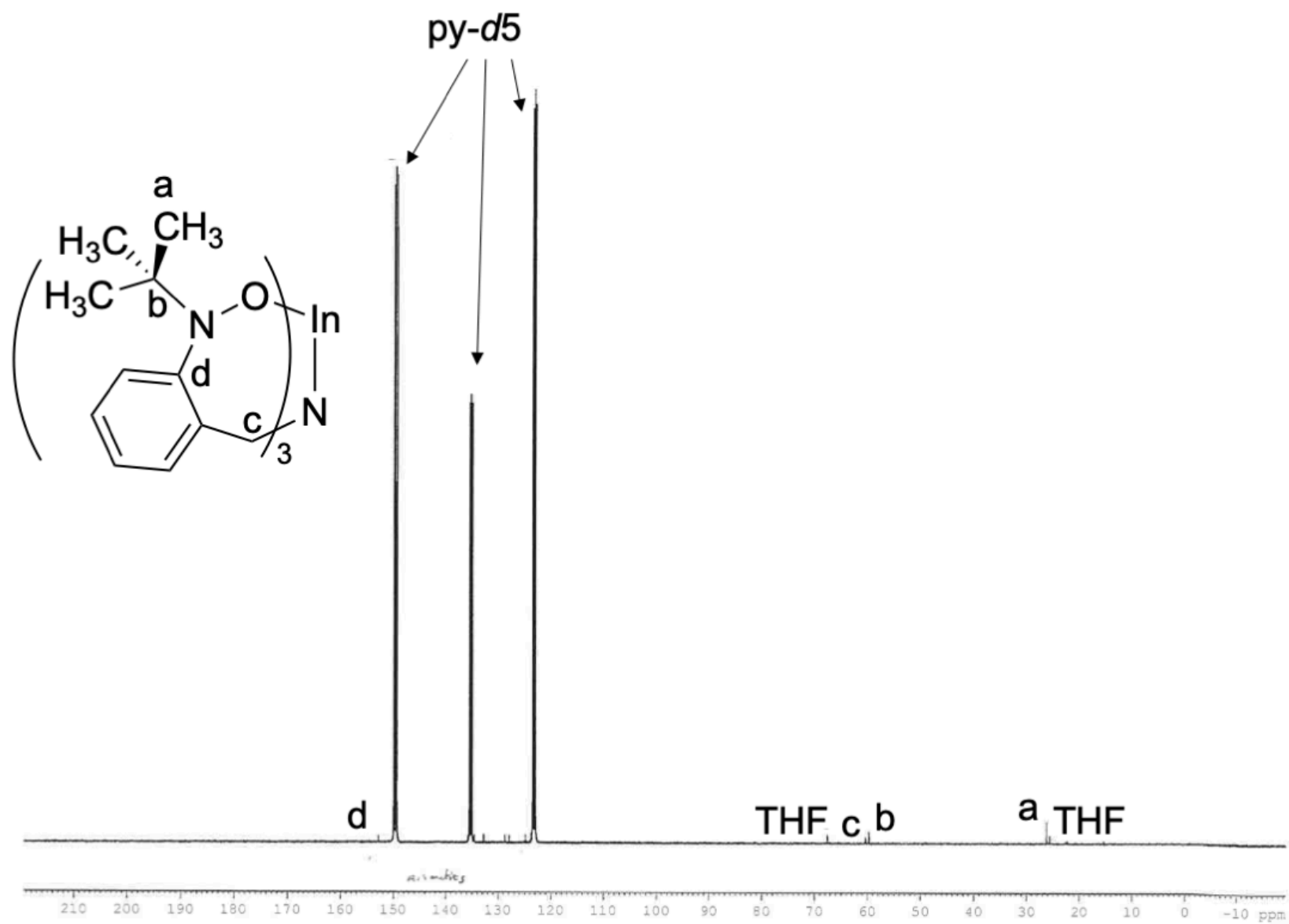


**Figure S6.**  $^{13}\text{C}\{^1\text{H}\}$  NMR spectrum of  $(\text{TriNOx}^3-)\text{In}$  (3) in  $\text{pyridine-}d_5$ .

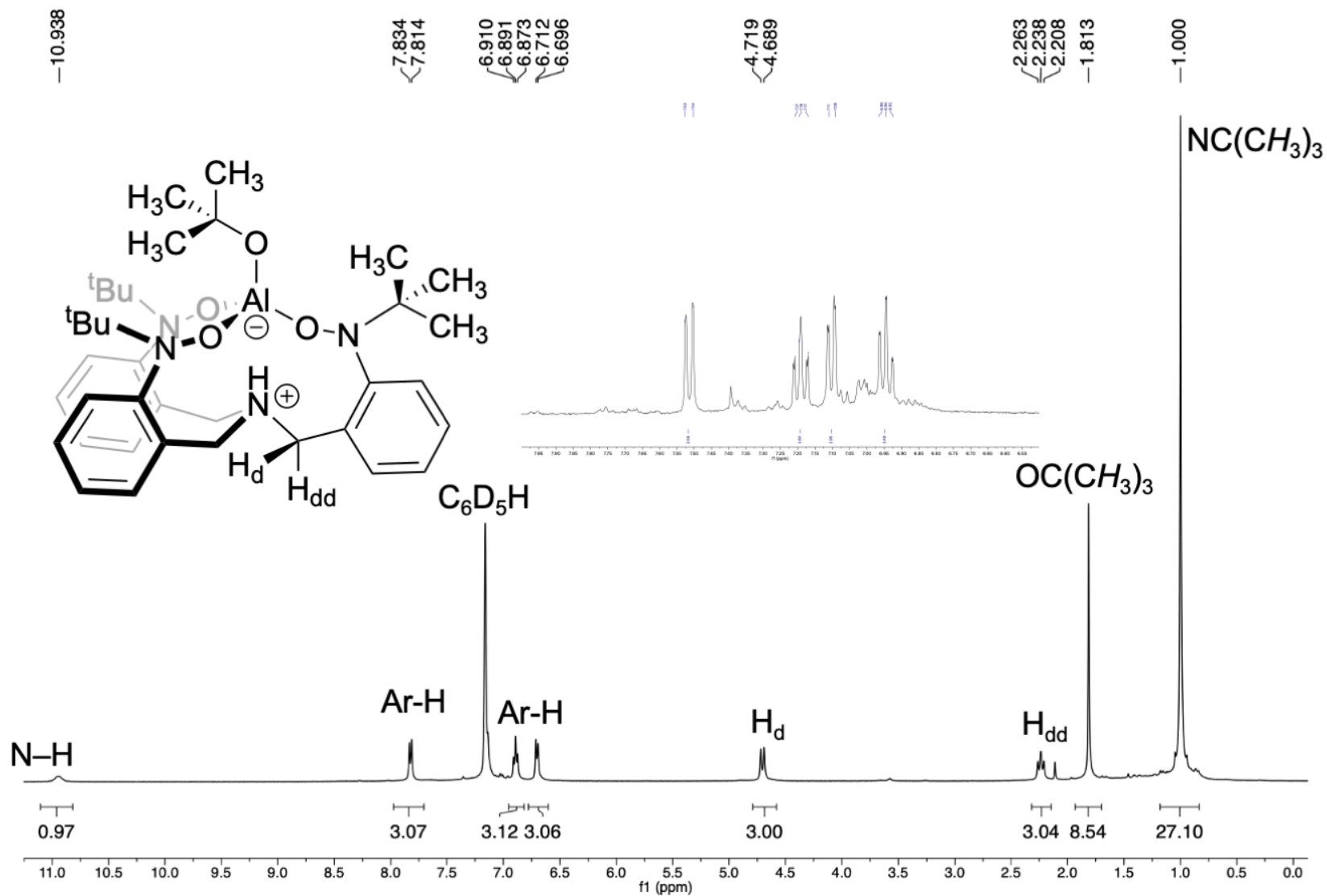


**Figure S7.** <sup>1</sup>H NMR spectrum of (HTriNOx<sup>2-</sup>)Al-O-Bu (**4**) in C<sub>6</sub>D<sub>6</sub>. The insert shows the aromatic region of the <sup>1</sup>H NMR of **4** in THF-*d*<sub>8</sub>.

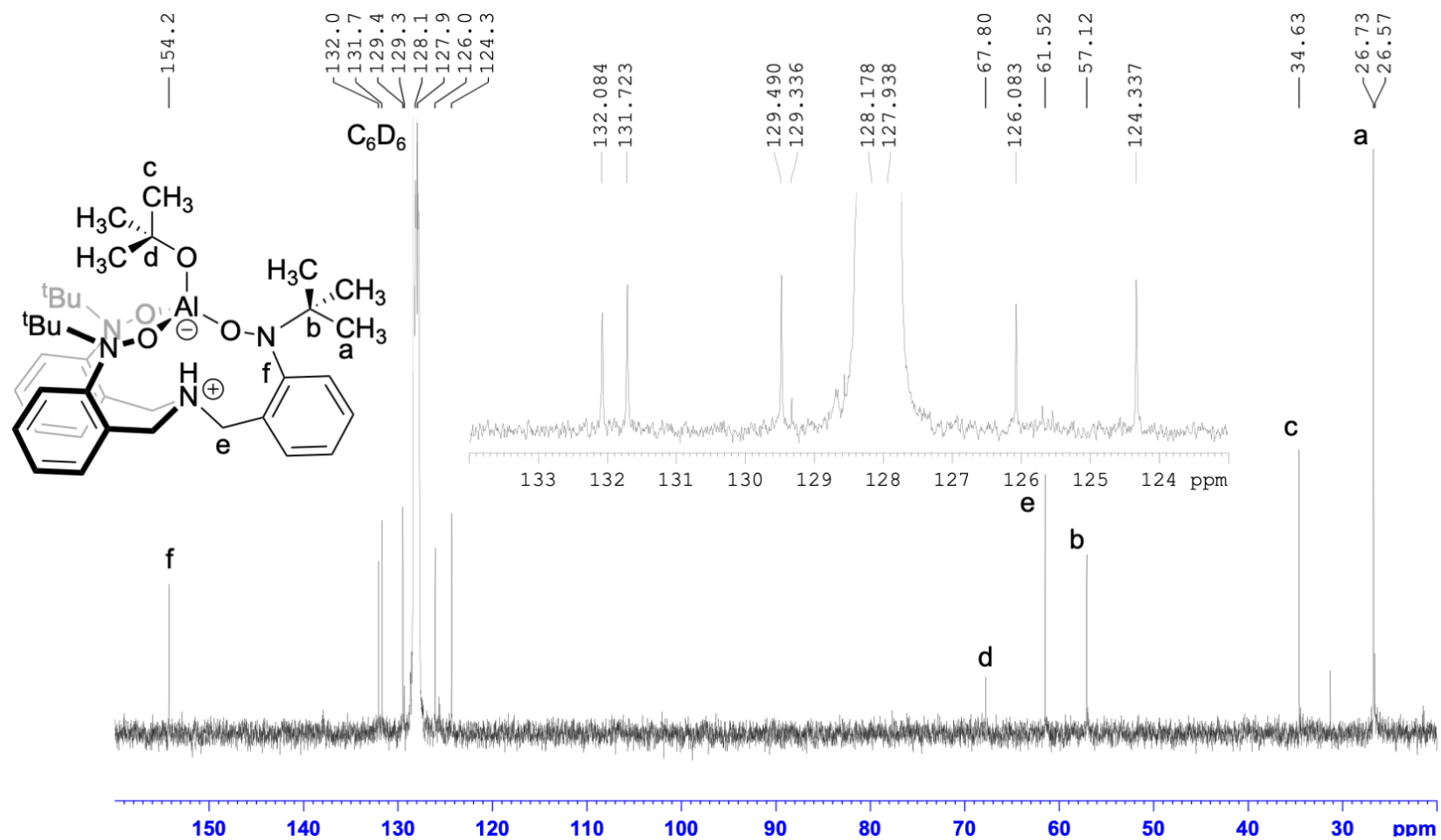


**Figure S8.** <sup>13</sup>C{<sup>1</sup>H} NMR spectrum of (HTriNOx<sup>2-</sup>)Al-O'Bu (4) in C<sub>6</sub>D<sub>6</sub>.

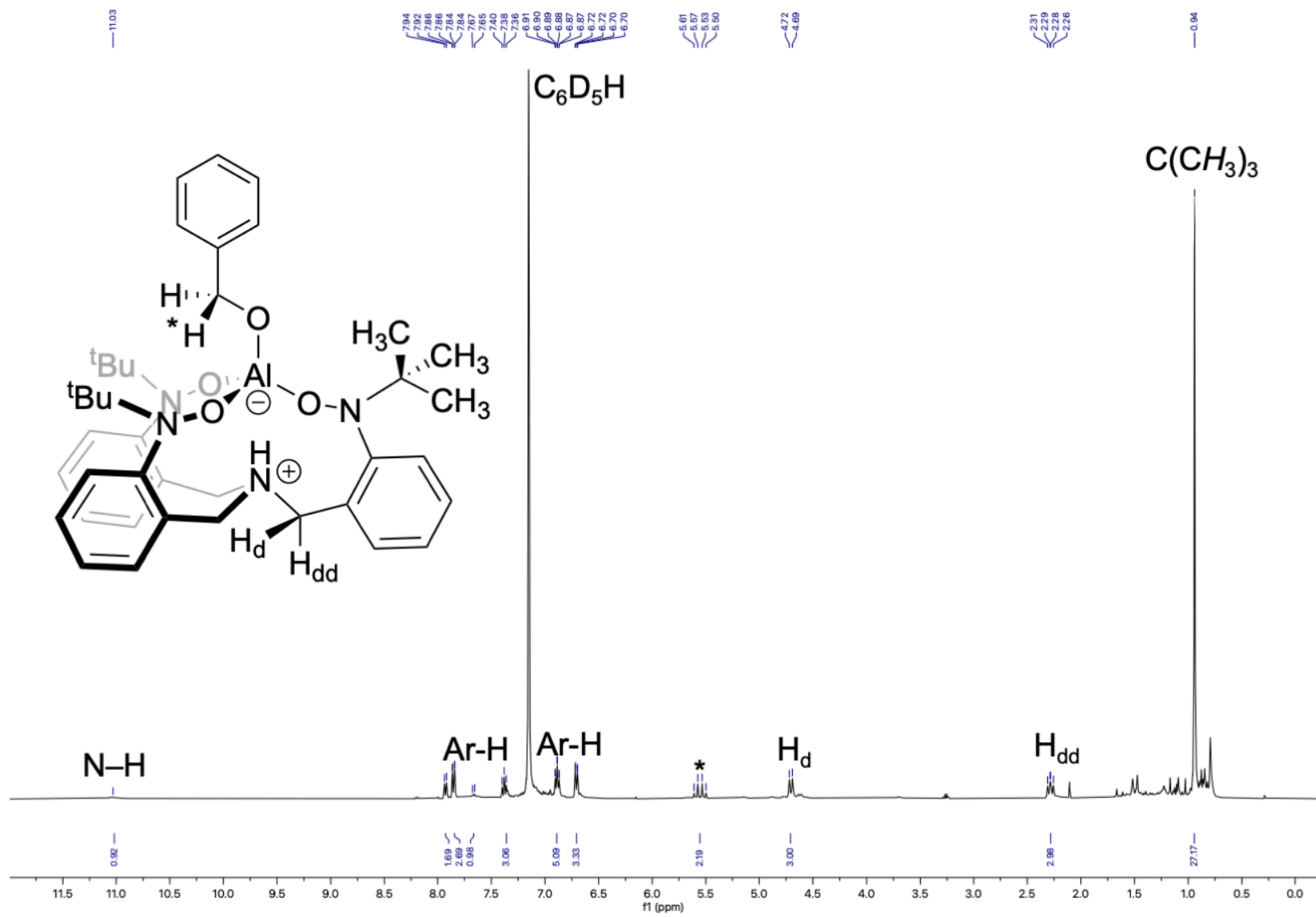


**Figure S9.**  $^1\text{H}$  NMR spectrum of  $(\text{HTriNOx}^2)\text{Al-OBn}$  (6) in  $\text{C}_6\text{D}_6$ .

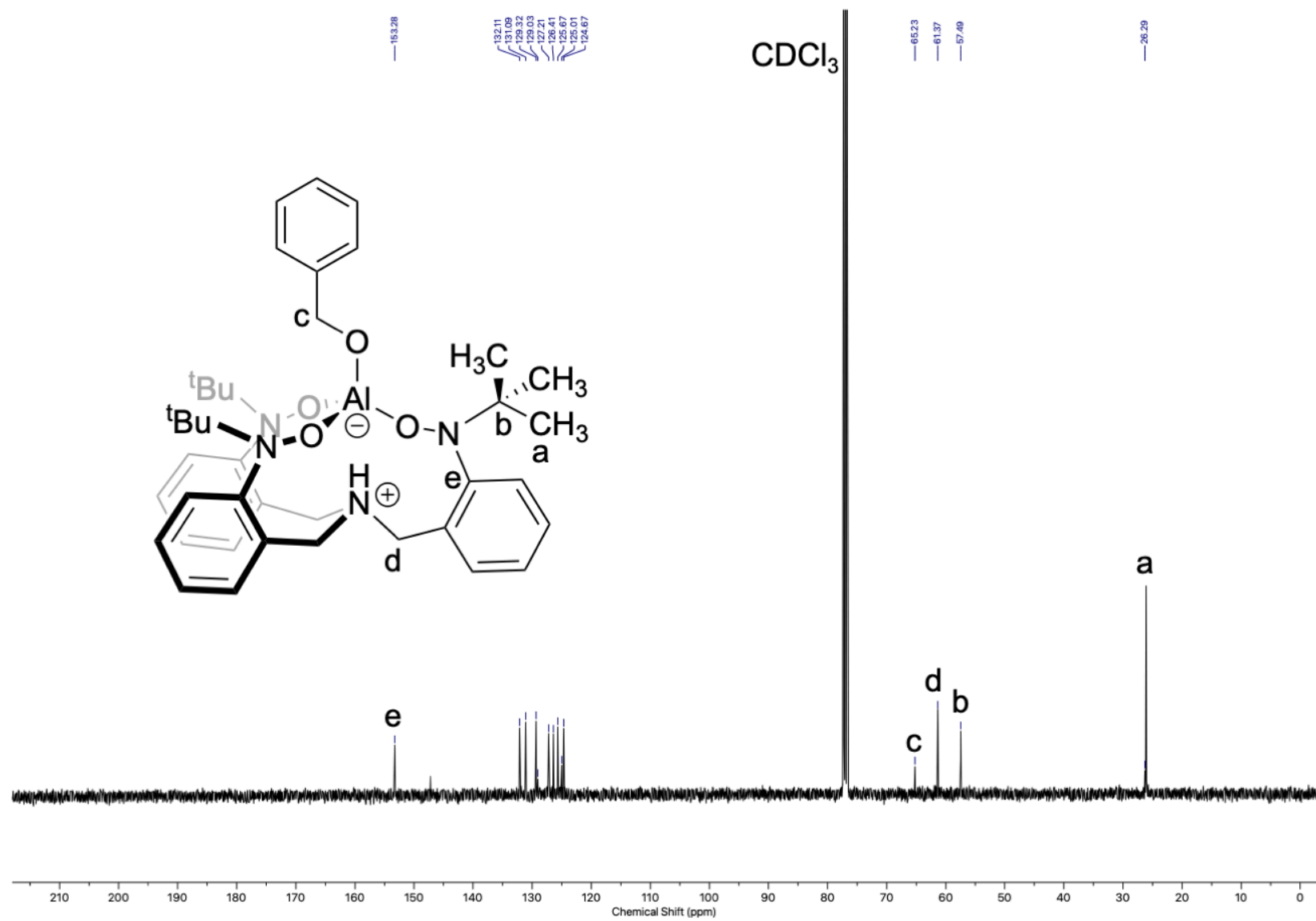


**Figure S10.** <sup>13</sup>C{<sup>1</sup>H} NMR spectrum of (HTriNOx<sup>2-</sup>)Al-OBn (**6**) in CDCl<sub>3</sub>.

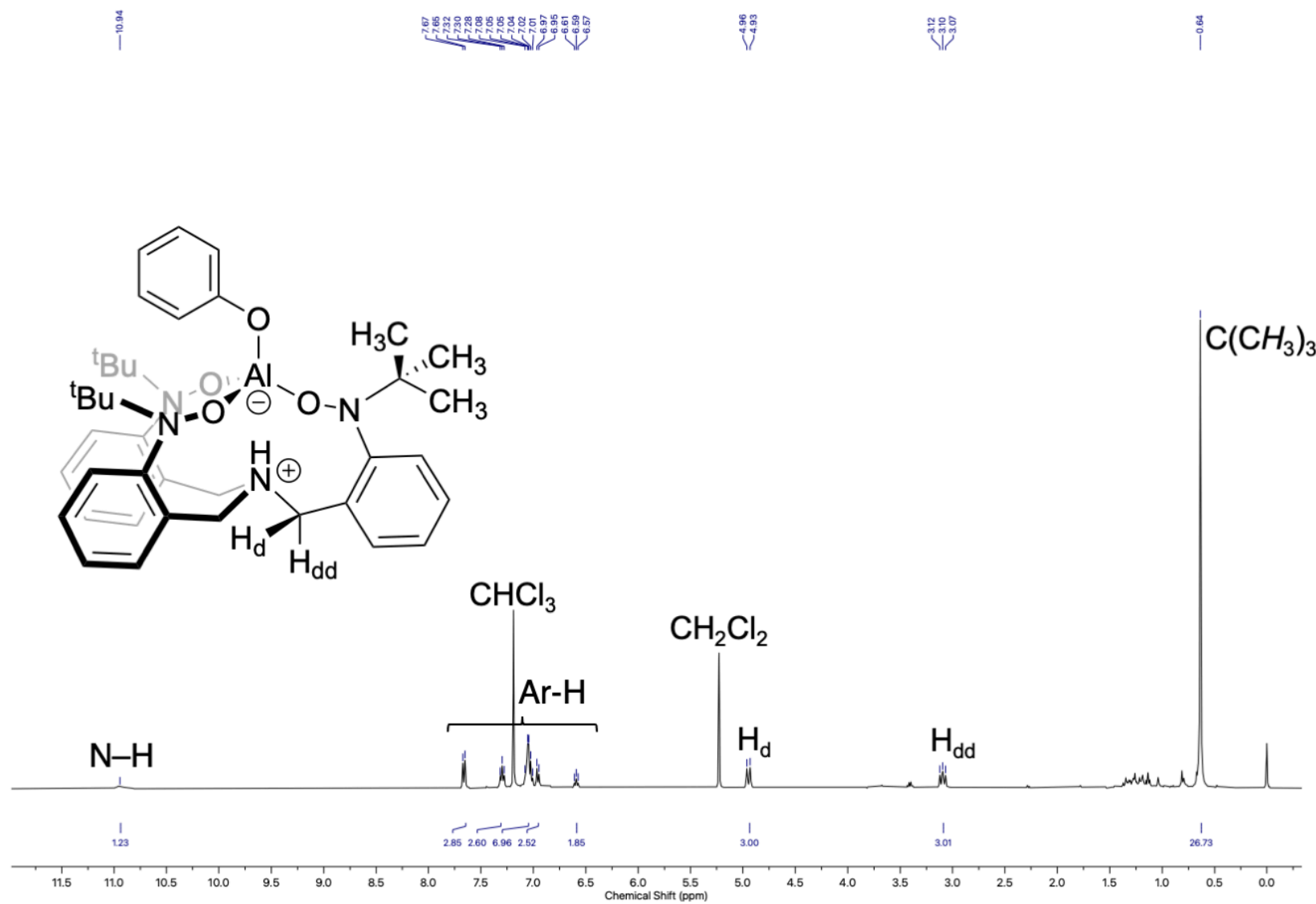


**Figure S11.** <sup>1</sup>H NMR spectrum of (HTriNOx<sup>2-</sup>)Al-OPh (**8**) in CDCl<sub>3</sub>.

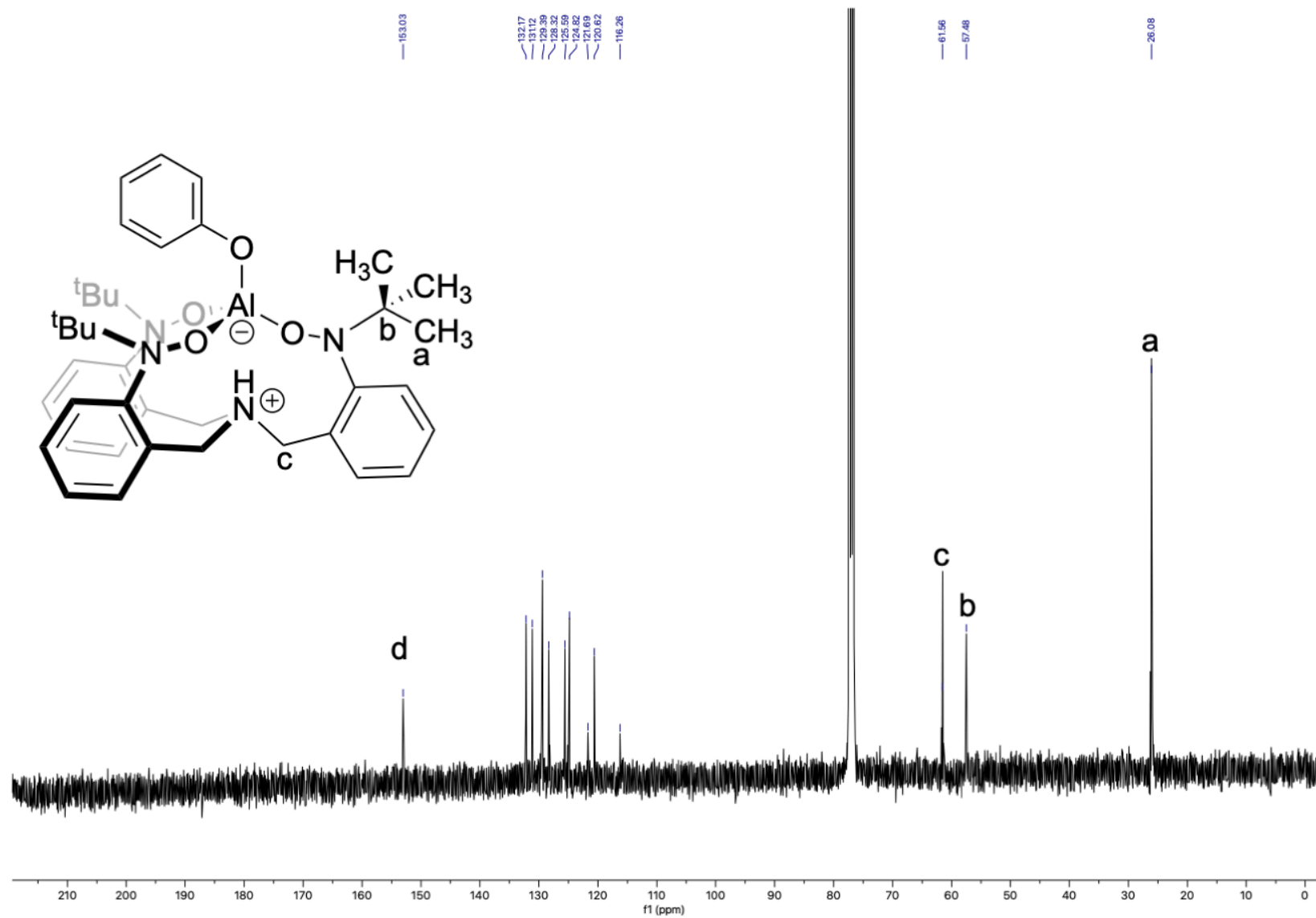


**Figure S12.** <sup>13</sup>C{<sup>1</sup>H} NMR spectrum of (HTriNOx<sup>2-</sup>)Al-OPh (**8**) in CDCl<sub>3</sub>.

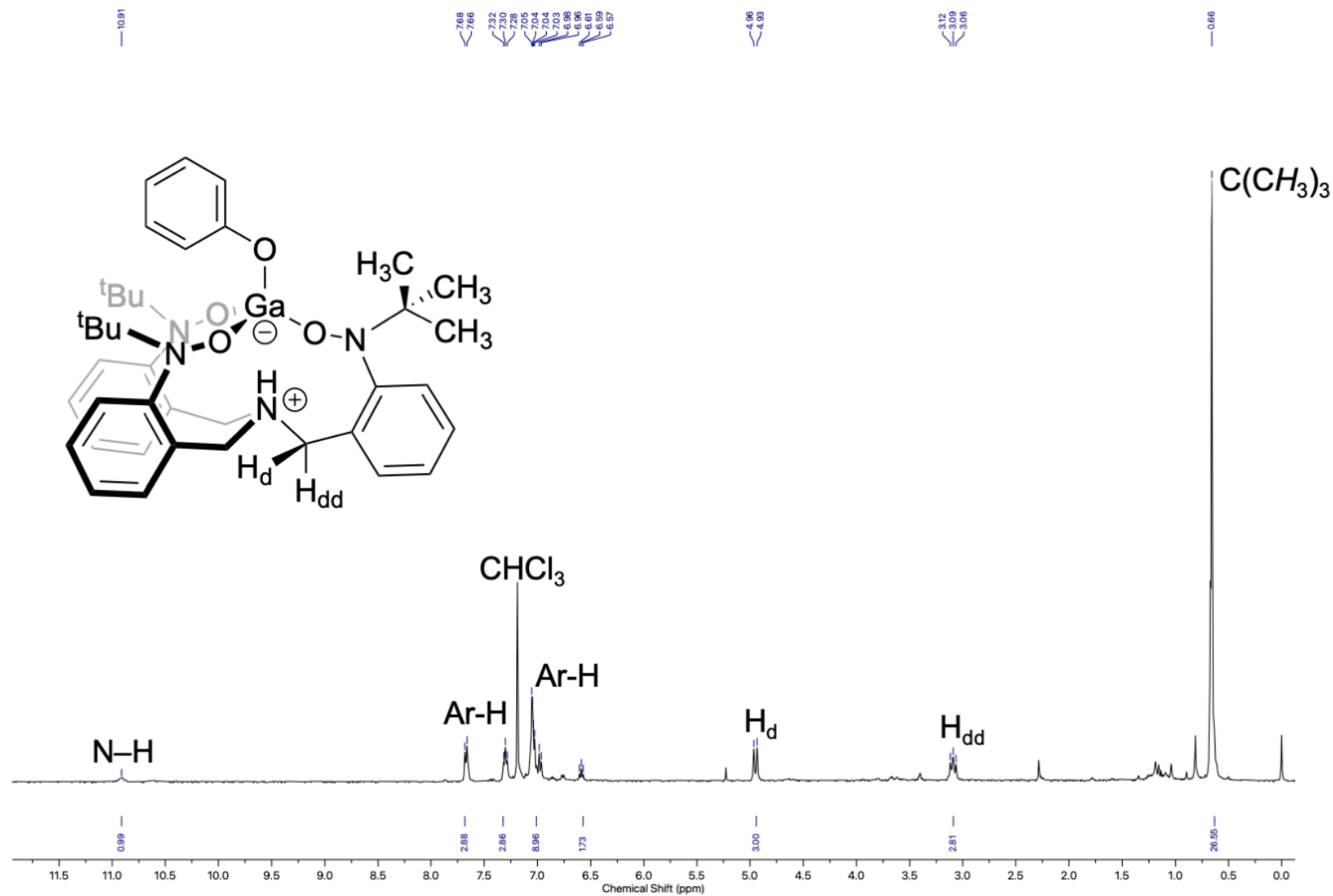


**Figure S13.** <sup>1</sup>H NMR spectrum of (HTriNOx<sup>2-</sup>)Ga-OPh (**9**) in CDCl<sub>3</sub>.



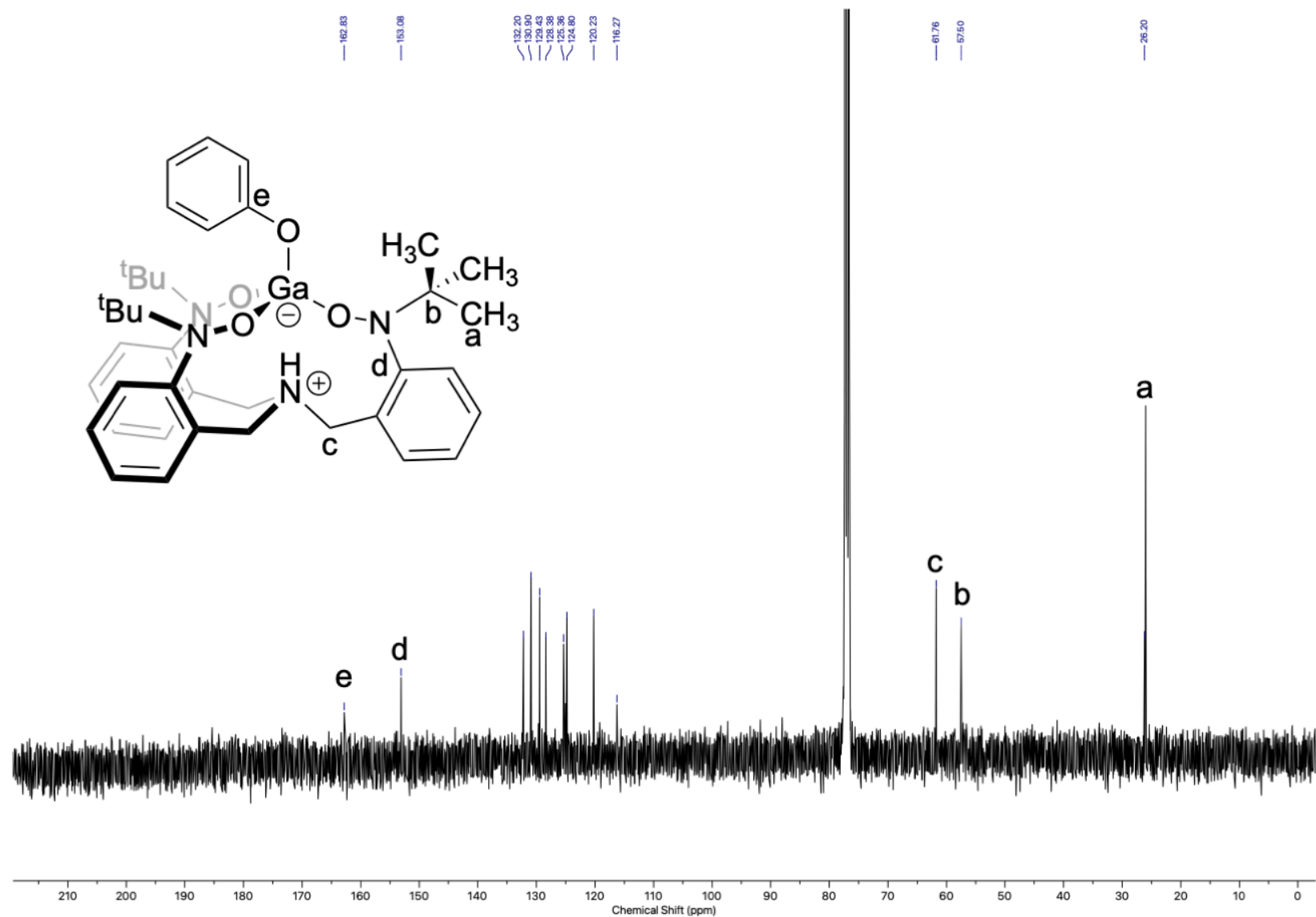


**Figure S14.**  $^{13}\text{C}\{^1\text{H}\}$  NMR spectrum of  $(\text{HTriNOx}^2-)\text{Ga-OPh}$  (**9**) in  $\text{CDCl}_3$ .

**Protocol for determination of the Lewis acid acceptor numbers for 1 and 2:** 0.25 mL of a 9 mM solution of either **1** or **2** ( $2.25 \times 10^{-3}$  mmol) in  $C_6D_6$  was added to a vial containing the given triethylphosphine chalcogenide ( $4.5 \times 10^{-3}$  mmol) in 0.25 mL of  $C_6D_6$ . The reactions were stirred for 30 min and then analyzed by  $^{31}P\{^1H\}$  NMR spectroscopy.

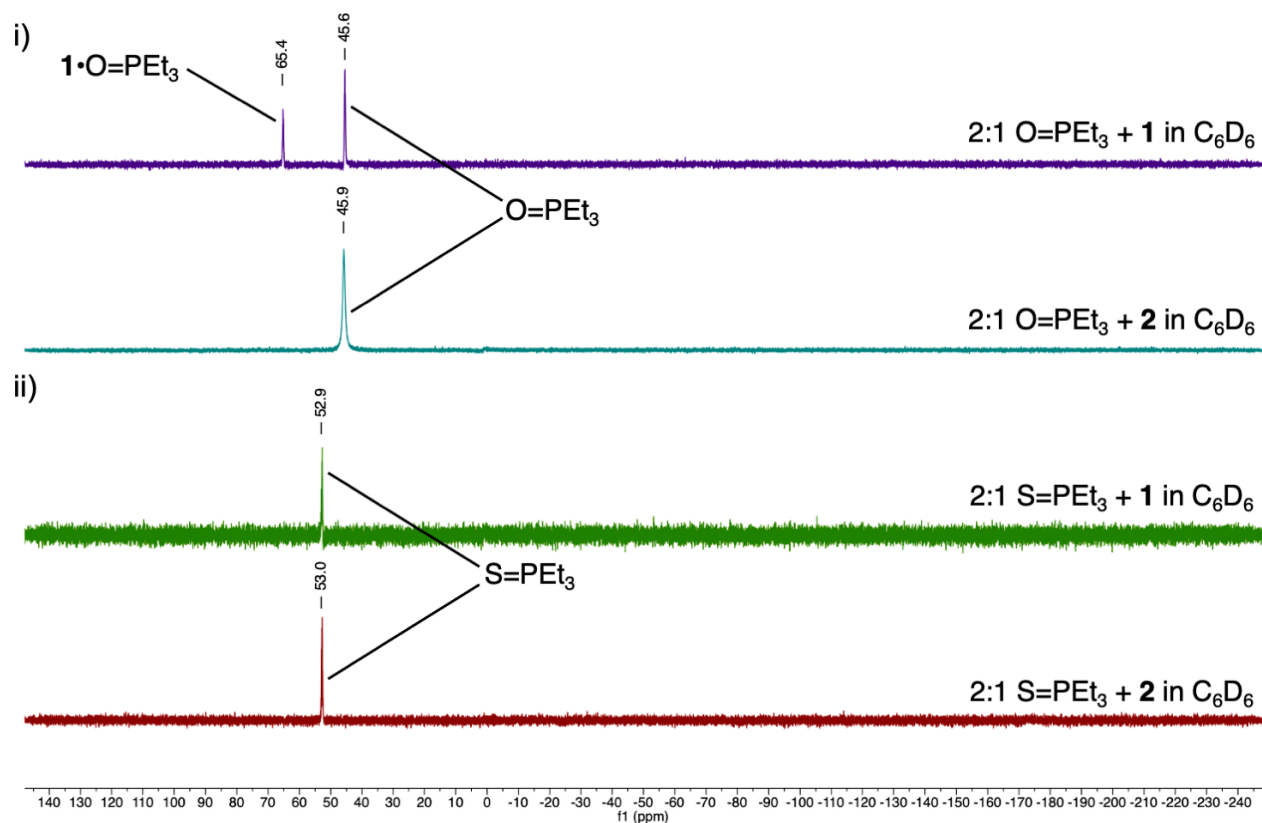


**Figure S15.** Stacked plot of the  $^{31}P\{^1H\}$  NMR spectra of the mixtures of Et<sub>3</sub>PO (i) and Et<sub>3</sub>PS (ii) experiments run to evaluate the Lewis acidity of complexes **1** and **2**.

**Protocol for the VT-NMR studies of Complexes 4, 6, and 8:** ~5 mg of complex was dissolved in ~0.75 mL of NMR solvent ( $C_6D_6$  for **4**;  $CDCl_3$  for **6** and **8**). The solution was transferred into an NMR tube equipped with a Teflon J. Young valve and the sample was allowed to equilibrate at 293 K and a  $^1H$  NMR spectrum was collected. Then,  $^1H$  NMR spectra were recorded at 303K, 313K, 323K, 333K, 343K, and 353K; before each collection, the sample was allowed to thermally equilibrate for 30 min and then the sample was shimmed prior to collection of the spectra.

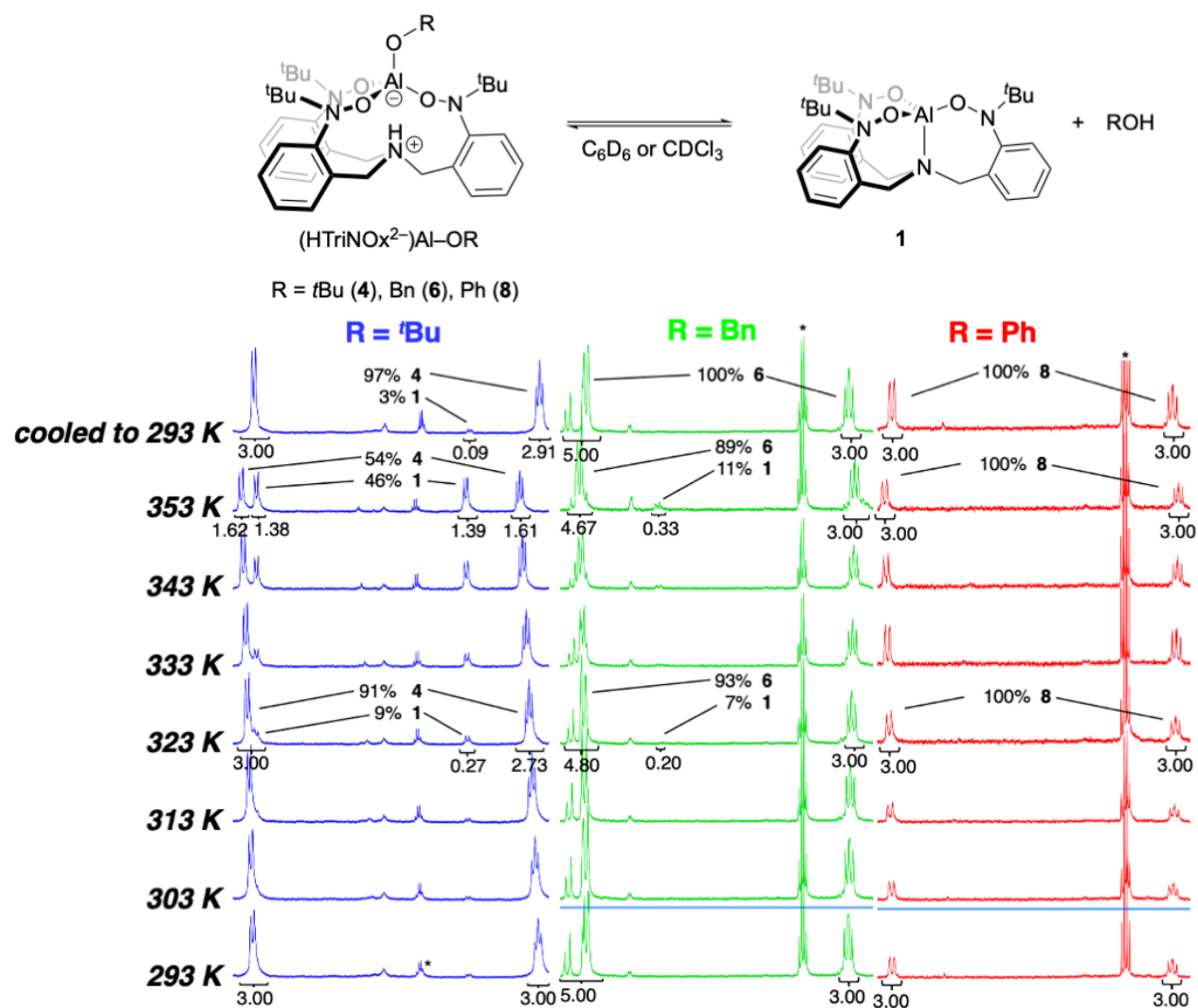


**Figure S16.** Diastereotopic proton region of the  $^1H$  NMR spectra of the **4**, **6**, and **8** complexes over the temperature range 293–353 K. The samples all contain diethyl ether (marked with an \*) that remains throughout the experiment.

**Protocol for the van't Hoff experiment of 1 + *t*BuOH:** Into a vial was added 500  $\mu\text{L}$  of a 9 mM stock solution of **1** in  $\text{C}_6\text{D}_6$  along with 125  $\mu\text{L}$  of a 6 mM stock solution of hexamethylcyclotrisiloxane as an internal standard, also in  $\text{C}_6\text{D}_6$ . Then, 125  $\mu\text{L}$  of a 36 mM solution of *tert*-butanol in  $\text{C}_6\text{D}_6$  was added and the reaction was allowed to stir at room temperature for 24 h. The reaction mixture was then transferred to a J-young capped NMR tube and loaded into the NMR spectrometer.  $^1\text{H}$  NMR spectra were collected at each indicated temperature. In all cases, the reaction was allowed to thermally equilibrate at the given temperature for 30 min prior to collection of the spectra. The concentration of the metal complexes **1** and **4** were determined by comparison of the integrations of the resonances for the *t*Bu and diastereotopic  $\text{CH}_2$  protons of the  $\text{TriNO}_x$  ligands in each complex relative to internal standard.  $K_{eq}$  values were calculated according to the formula:

$$K_{eq} = \frac{[4]}{[1][tBuOH]} \quad (\text{Eq. S1})$$

**Protocol for the determining the  $K_{eq}$  values for the reactions of 2 with alcohols.** For each experiment, 500  $\mu\text{L}$  of a 9 mM stock solution of **2** in  $\text{CDCl}_3$  was dispensed into a vial along with 125  $\mu\text{L}$  of a 6 mM stock solution of hexamethylcyclotrisiloxane as an internal standard also in  $\text{CDCl}_3$ . Then, 125  $\mu\text{L}$  of a 36 mM stock solution of the appropriate alcohol in  $\text{CDCl}_3$  was dispensed into the vial. The reaction was allowed to stir at room temperature for 24 hours after which the reaction was transferred to an NMR tube and analyzed by  $^1\text{H}$  NMR spectroscopy.  $K_{eq}$  values were calculated according to the formula:

$$K_{eq} = \frac{[(HTriNO_x)MOR]}{[2][ROH]} \quad (\text{Eq. S2})$$

The concentration of the metal complexes were determined by comparison of the integrations of the ligand NMR signatures to internal standard. For **2** the concentration was taken as the average value determined from comparison to the *t*Bu groups as well as both diastereotopic protons of the bridgehead  $\text{CH}_2$  groups. The concentration of the  $(\text{HTriNO}_x^{2-})\text{Ga-OR}$  complexes were similarly determined by the average of the value found for the *t*Bu groups as well as both diastereotopic protons of the bridgehead  $\text{CH}_2$  groups, as well as with any easily identifiable NMR handles in the R group of the resultant alkoxide ligand. The concentration of unreacted alcohol was assumed to be equal to that unreacted complex **2**.

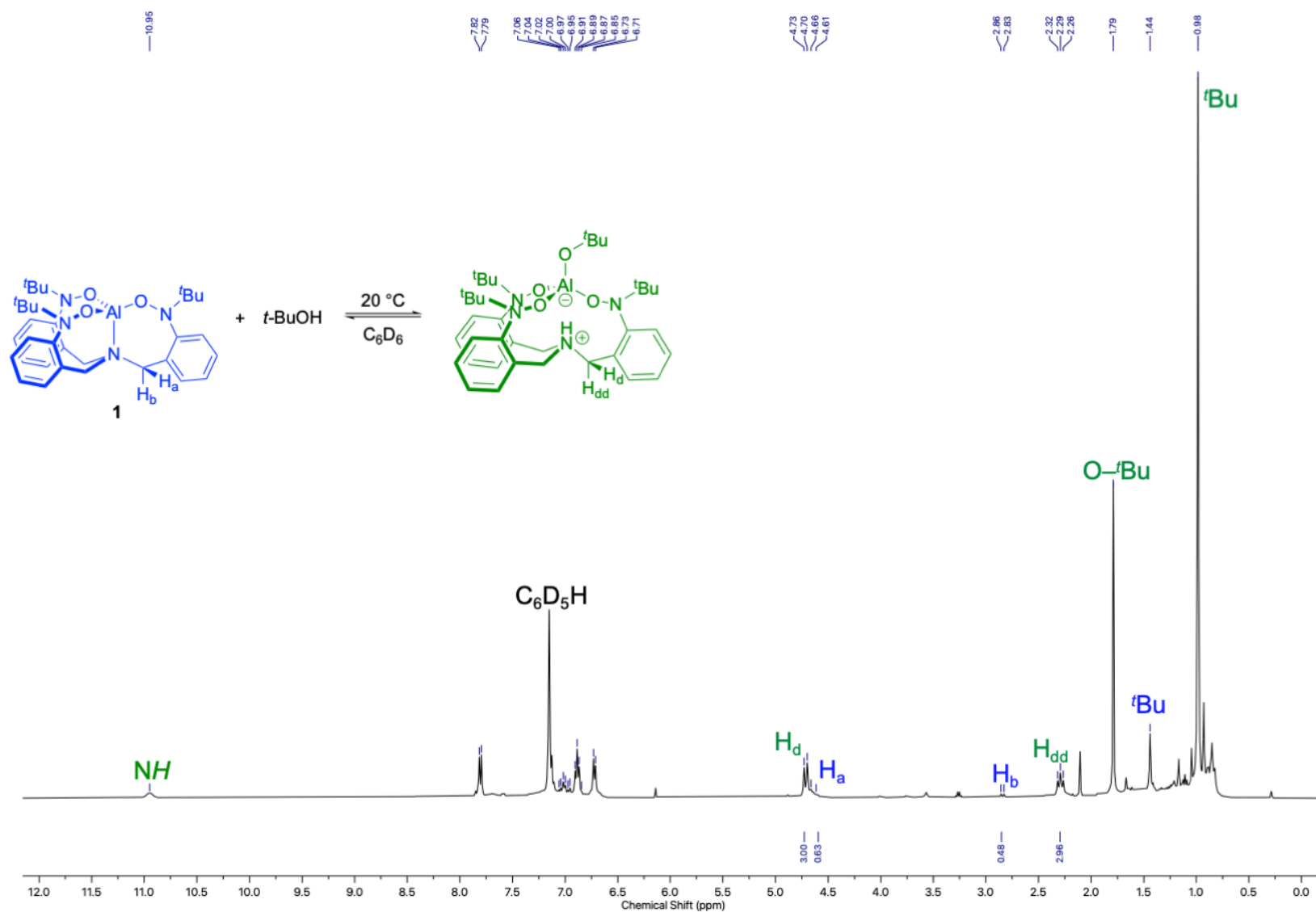


**Figure S17.**  $^1\text{H}$  NMR spectrum of a 1:1 mixture of **1**:*t*-BuOH. Taken in  $\text{C}_6\text{D}_6$  and recorded after 24 hours of stirring at room temperature.

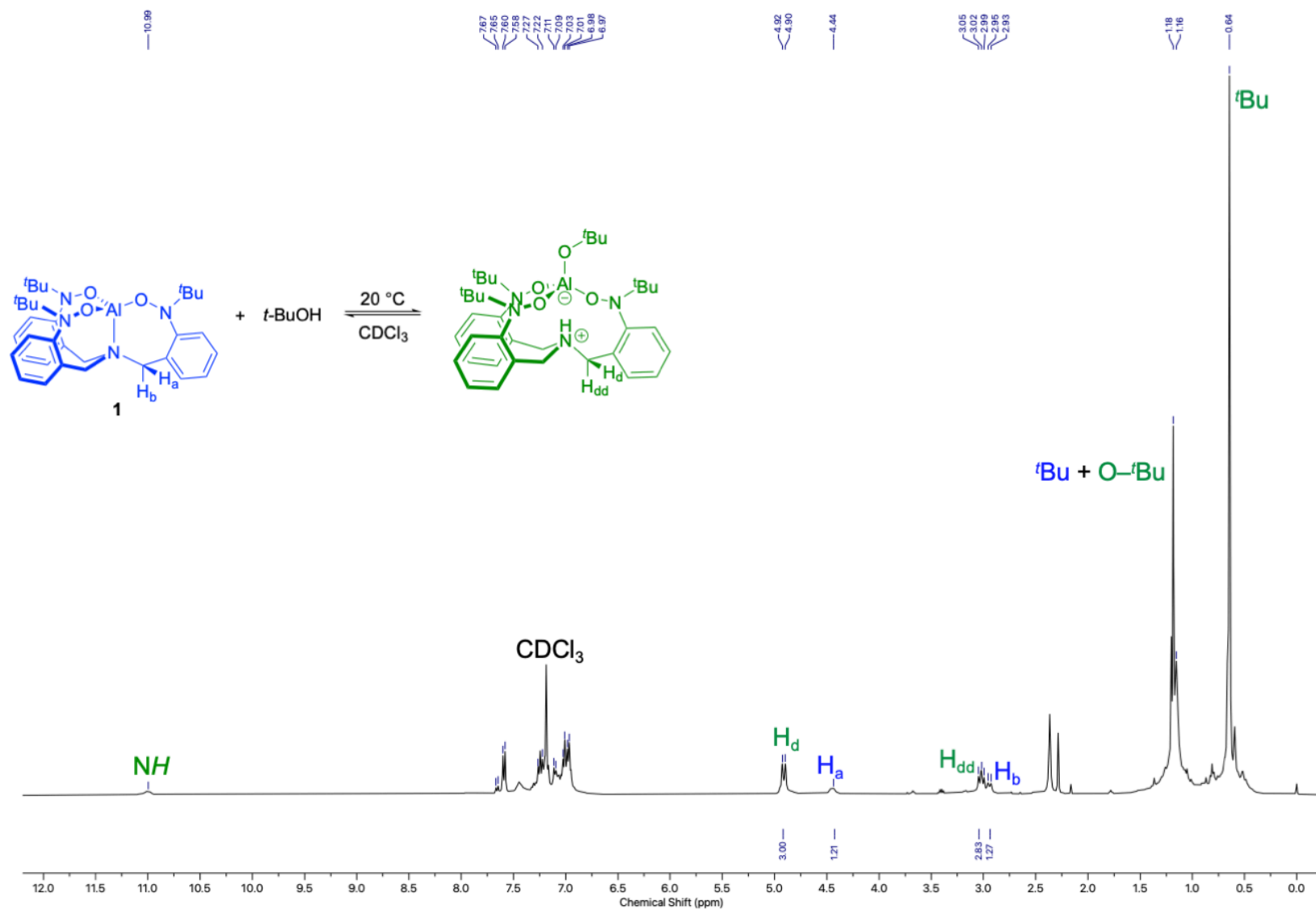


**Figure S18.**  $^1\text{H}$  NMR spectrum of a 1:1 mixture of **1**:*t*-BuOH. Taken in  $\text{CDCl}_3$  and recorded after 24 hours of stirring at room temperature.

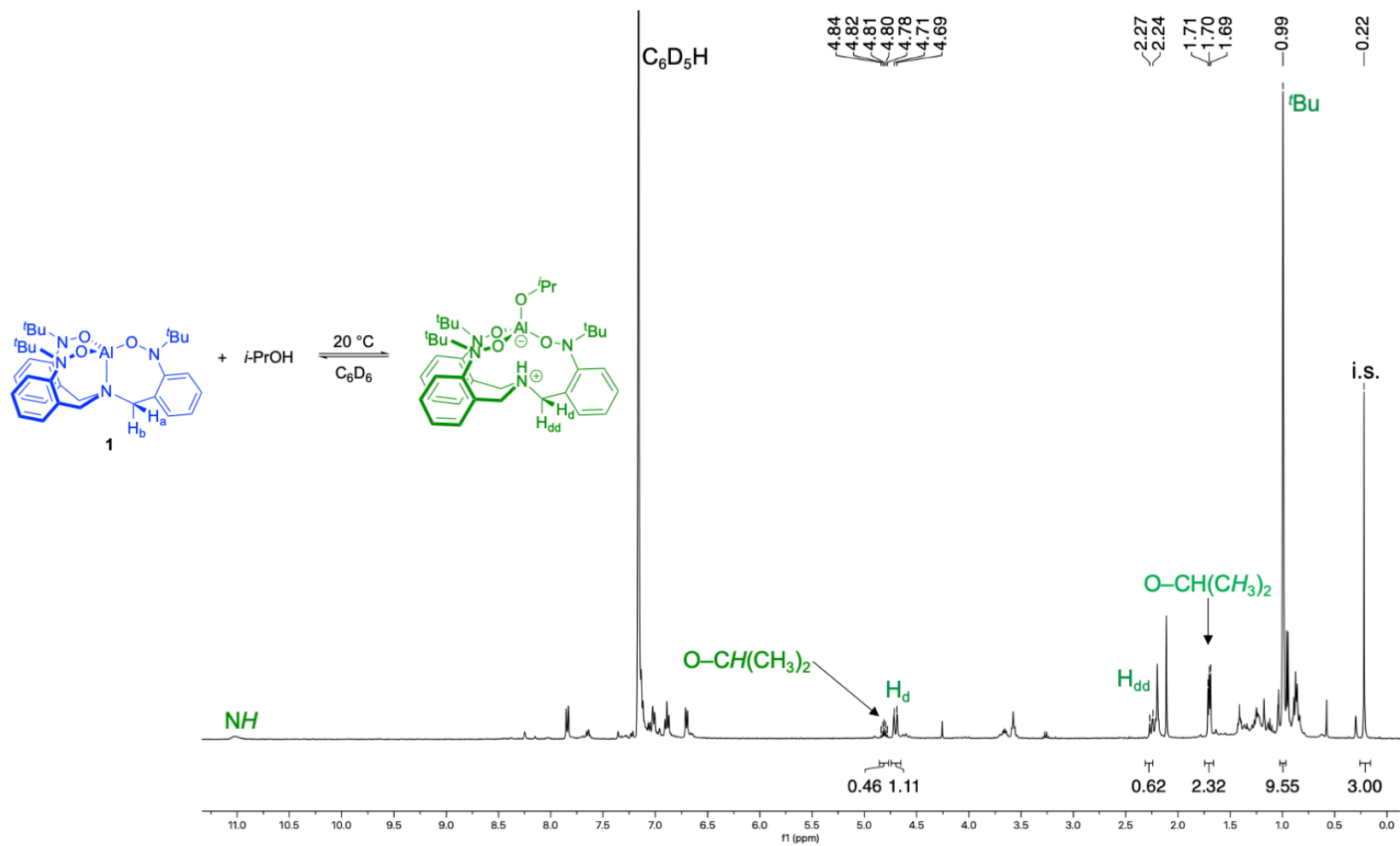


**Figure S19.**  $^1\text{H}$  NMR spectrum of a 1:1 mixture of **1**:*i*-PrOH. Taken in  $C_6D_6$  and recorded after 24 hours of stirring at room temperature.

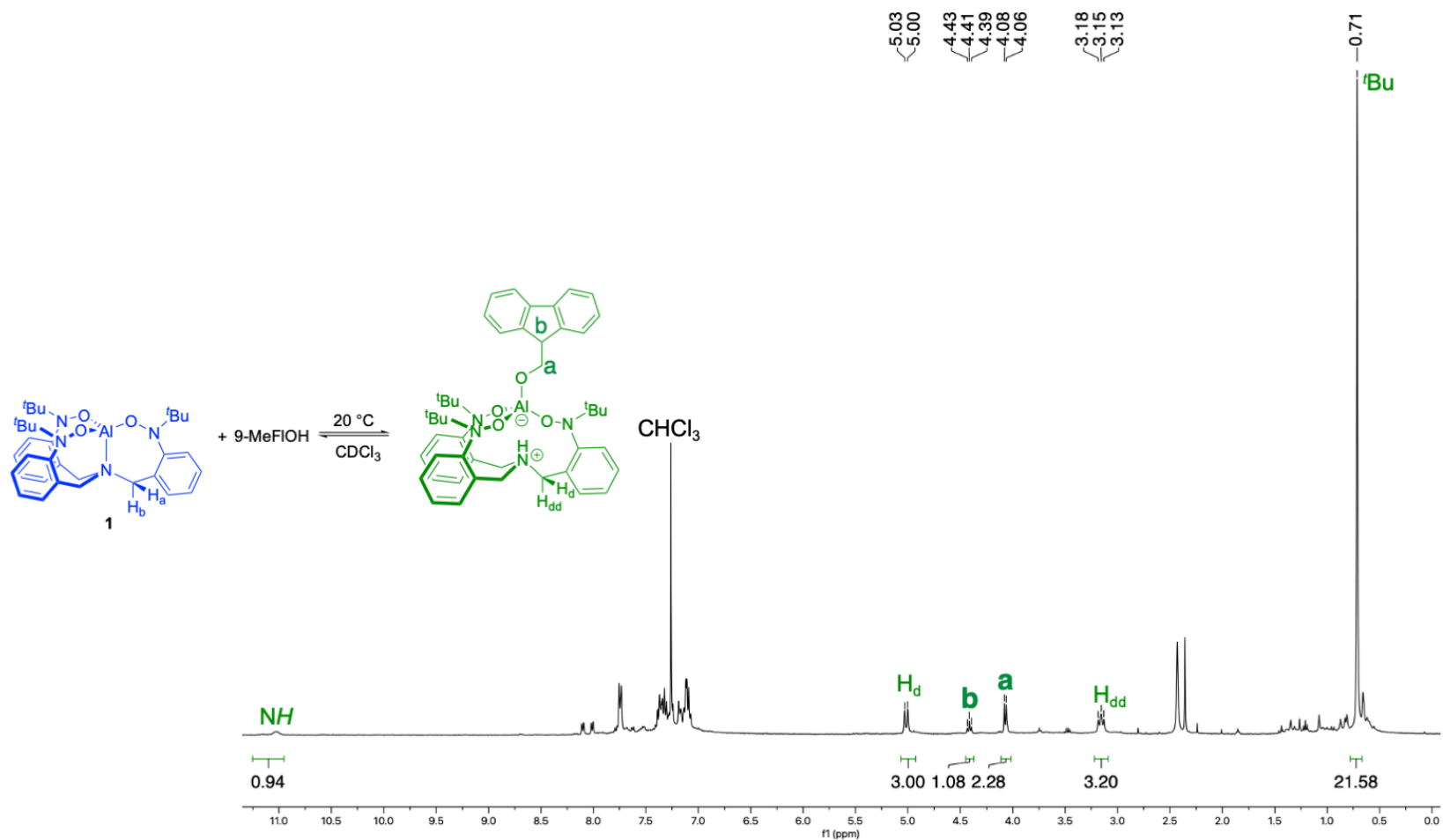


**Figure S20.**  $^1\text{H}$  NMR spectrum of a 1:1 mixture of **1**:9-fluorene-9-ylmethanol. Taken in  $\text{CDCl}_3$  and recorded after 24 hours of stirring at room temperature.



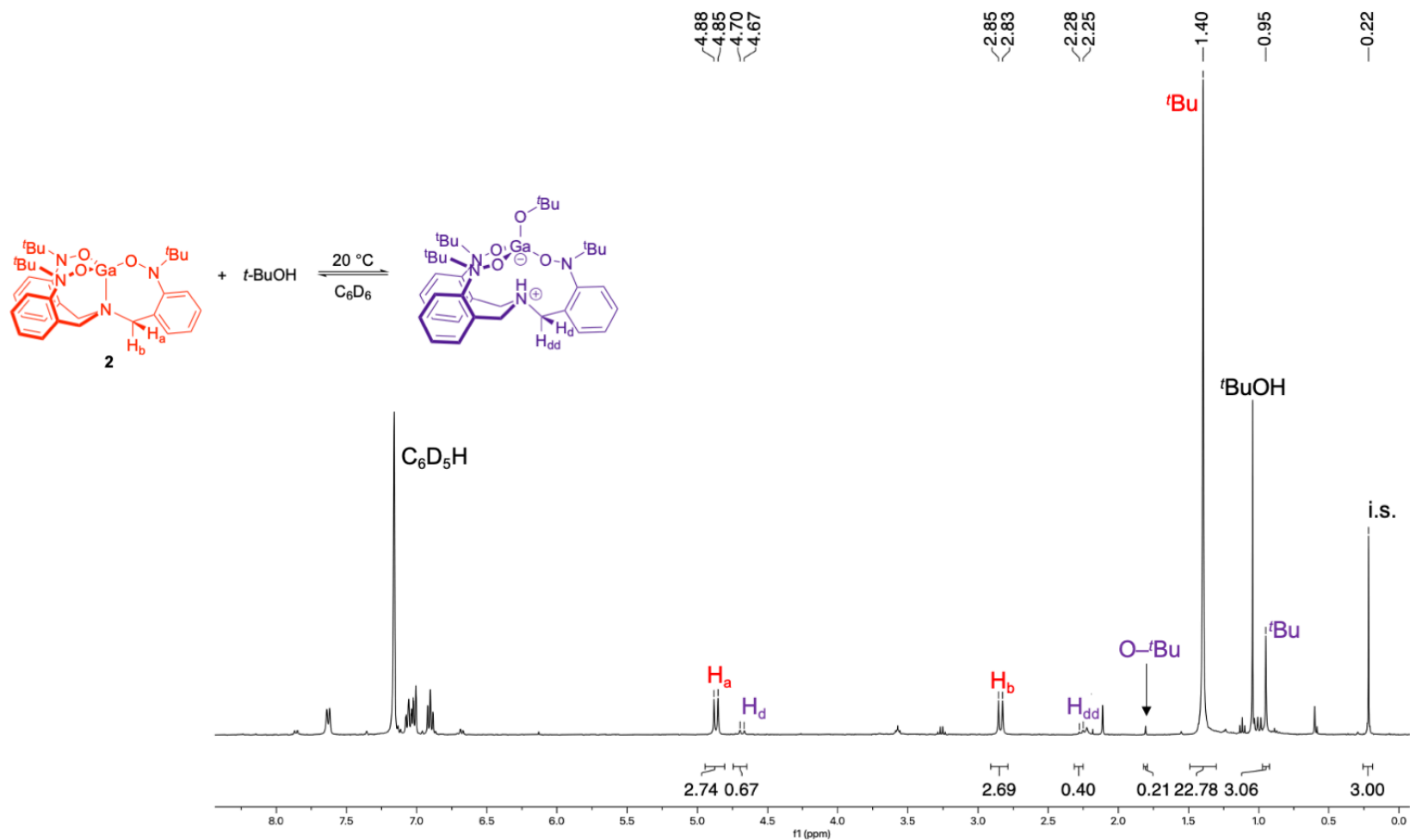


**Figure S21.**  $^1H$  NMR spectrum of a 1:1 mixture of **2**:*t*-BuOH. Taken in  $C_6D_6$  and recorded after 24 hours of stirring at room temperature (Table 1, entry 1).

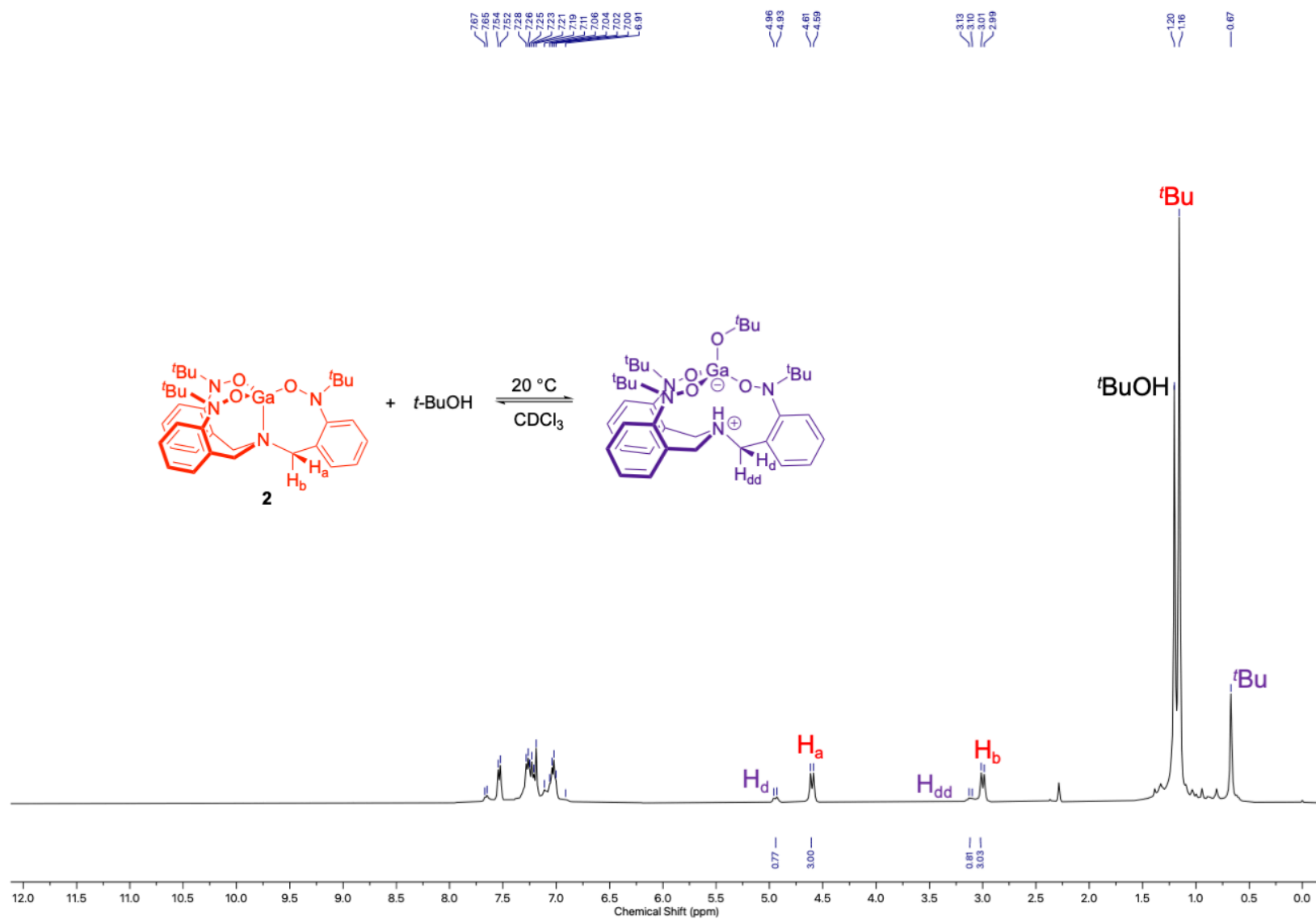


**Figure S22.**  $^1\text{H}$  NMR spectrum of a 1:1 mixture of **2**: $t\text{-BuOH}$ . Taken in  $\text{CDCl}_3$  and recorded after 24 hours of stirring at room temperature.

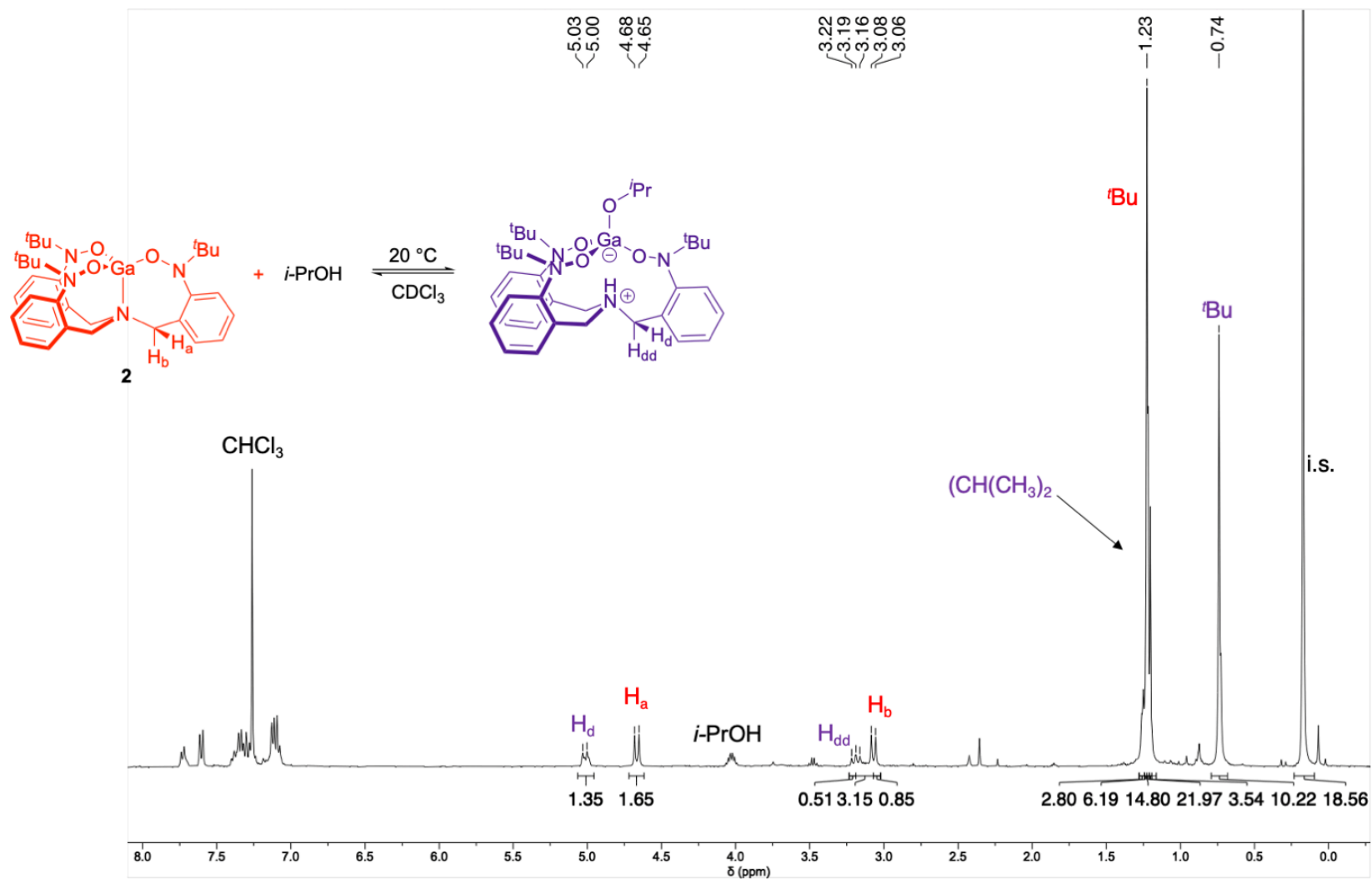


**Figure S23.**  $^1\text{H}$  NMR spectrum of a 1:1 mixture of **2**:*i*-PrOH. Taken in  $\text{CDCl}_3$  and recorded after 24 hours of stirring at room temperature (Table 1, entry 2).

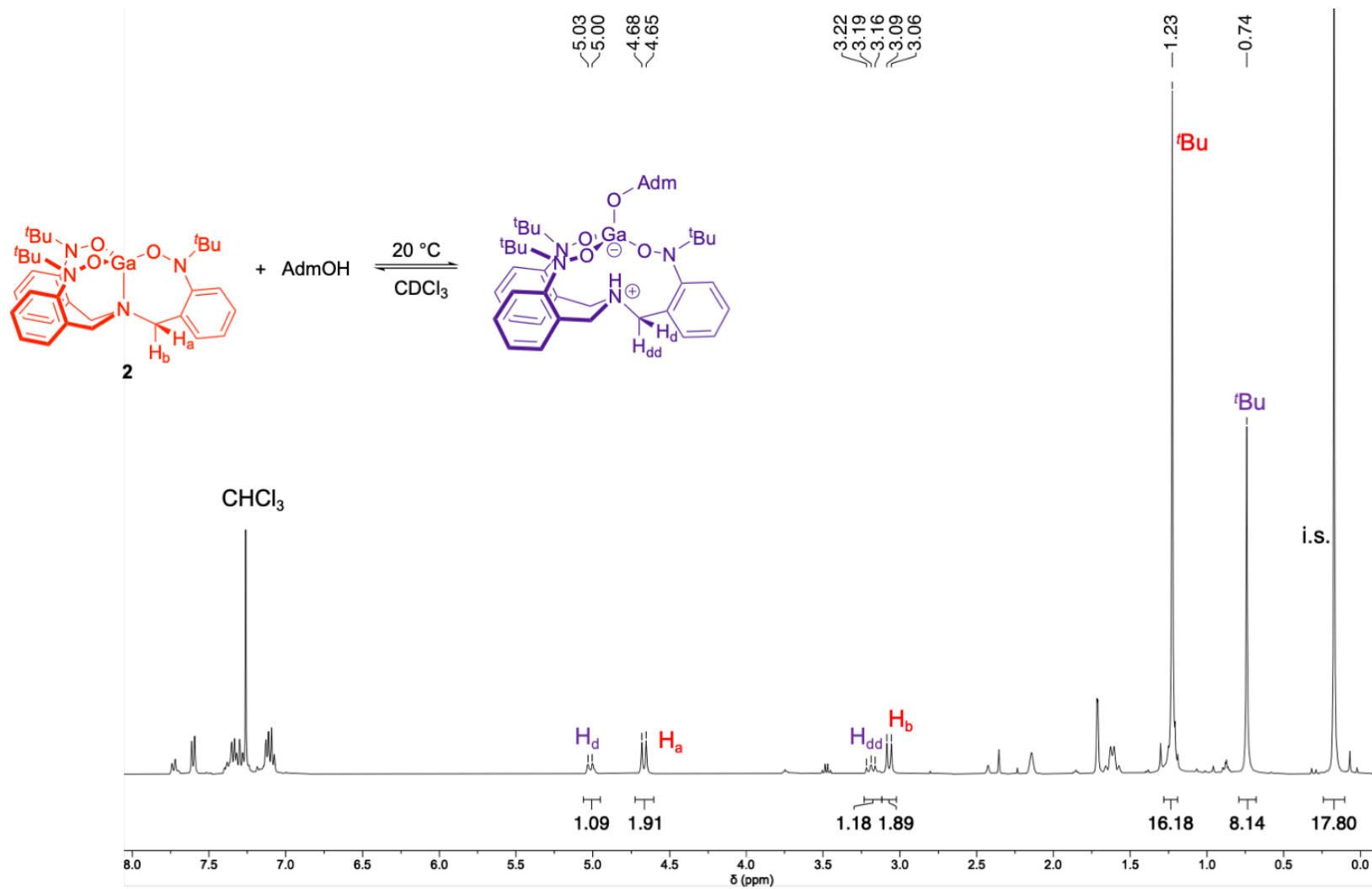


**Figure S24.**  $^1\text{H}$  NMR spectrum of a 1:1 mixture of **2**:1-adamantanol. Taken in  $\text{CDCl}_3$  and recorded after 24 hours of stirring at room temperature (Table 1, entry 3).

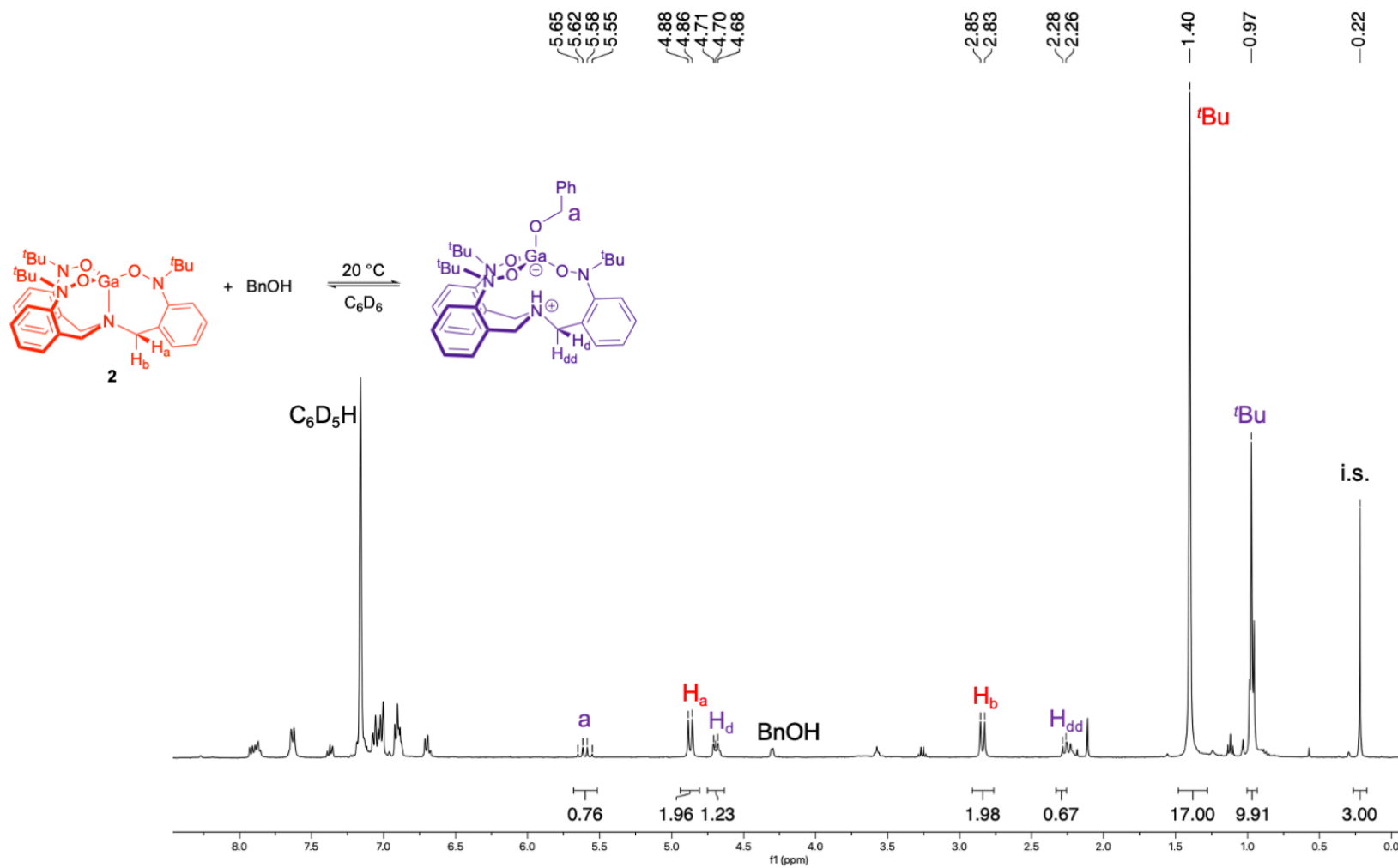


**Figure S25.**  $^1H$  NMR spectrum of a 1:1 mixture of **2**:BnOH. Taken in  $C_6D_6$  and recorded after 24 hours of stirring at room temperature (Table 1, entry 4).

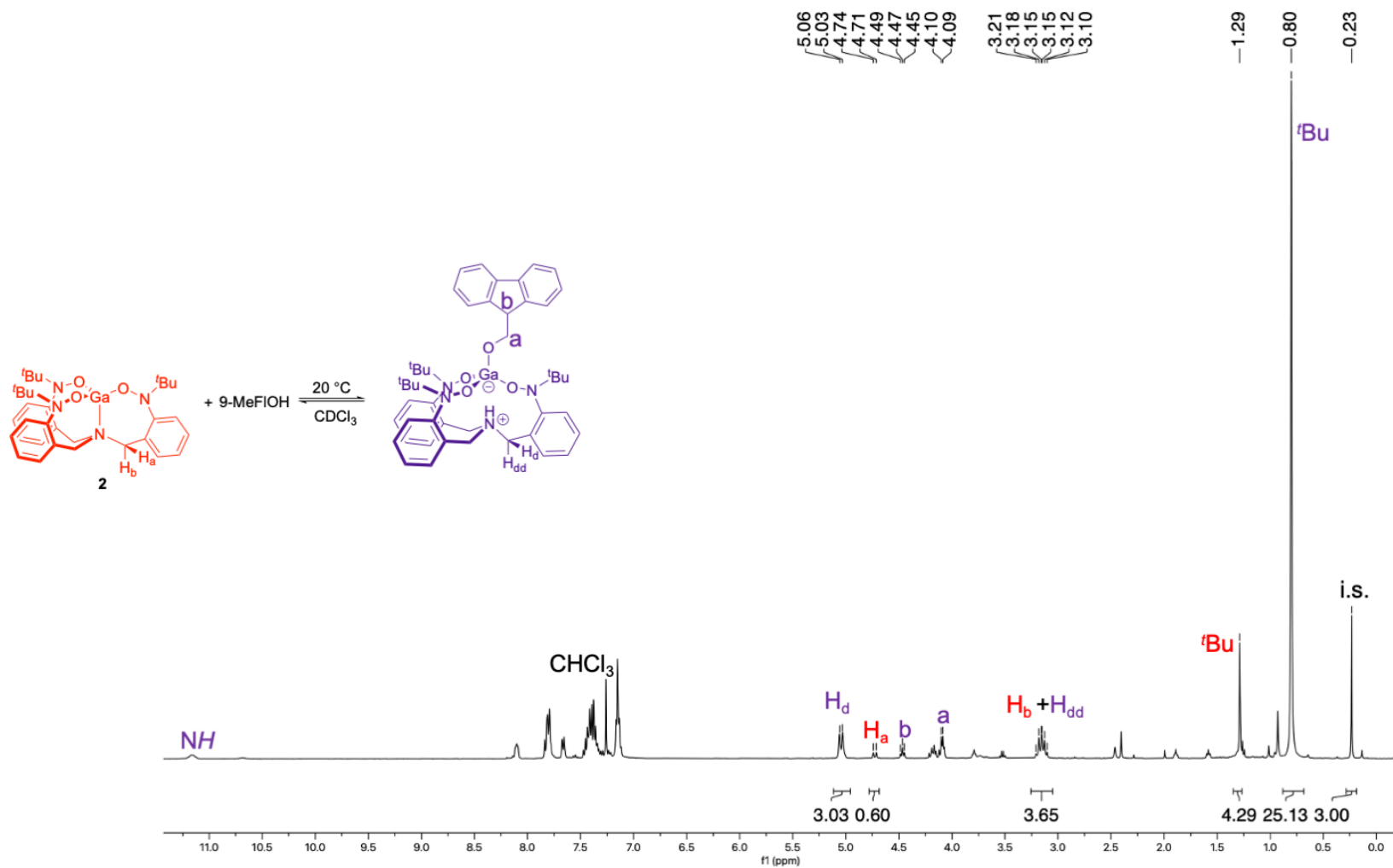


**Figure S26.** <sup>1</sup>H NMR spectrum of a 1:1 mixture of **2**:9-fluorenemethanol. Taken in CDCl<sub>3</sub> and recorded after 24 hours of stirring at room temperature (Table 1, entry 5).

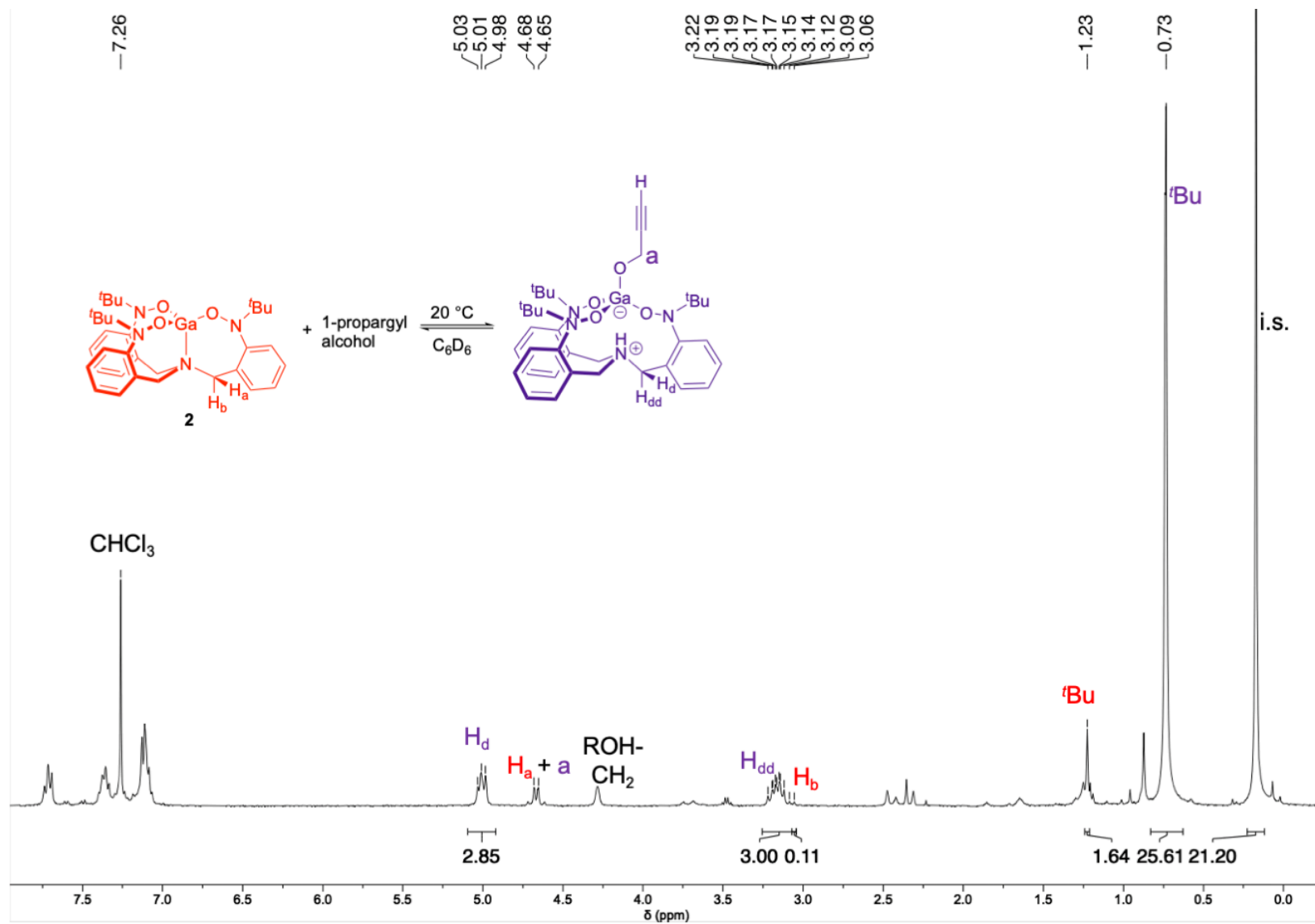


**Figure S27.**  $^1H$  NMR spectrum of a 1:1 mixture of **2**:propargyl alcohol. Taken in  $CDCl_3$  and recorded after 24 hours of stirring at room temperature (Table 1, entry 6).

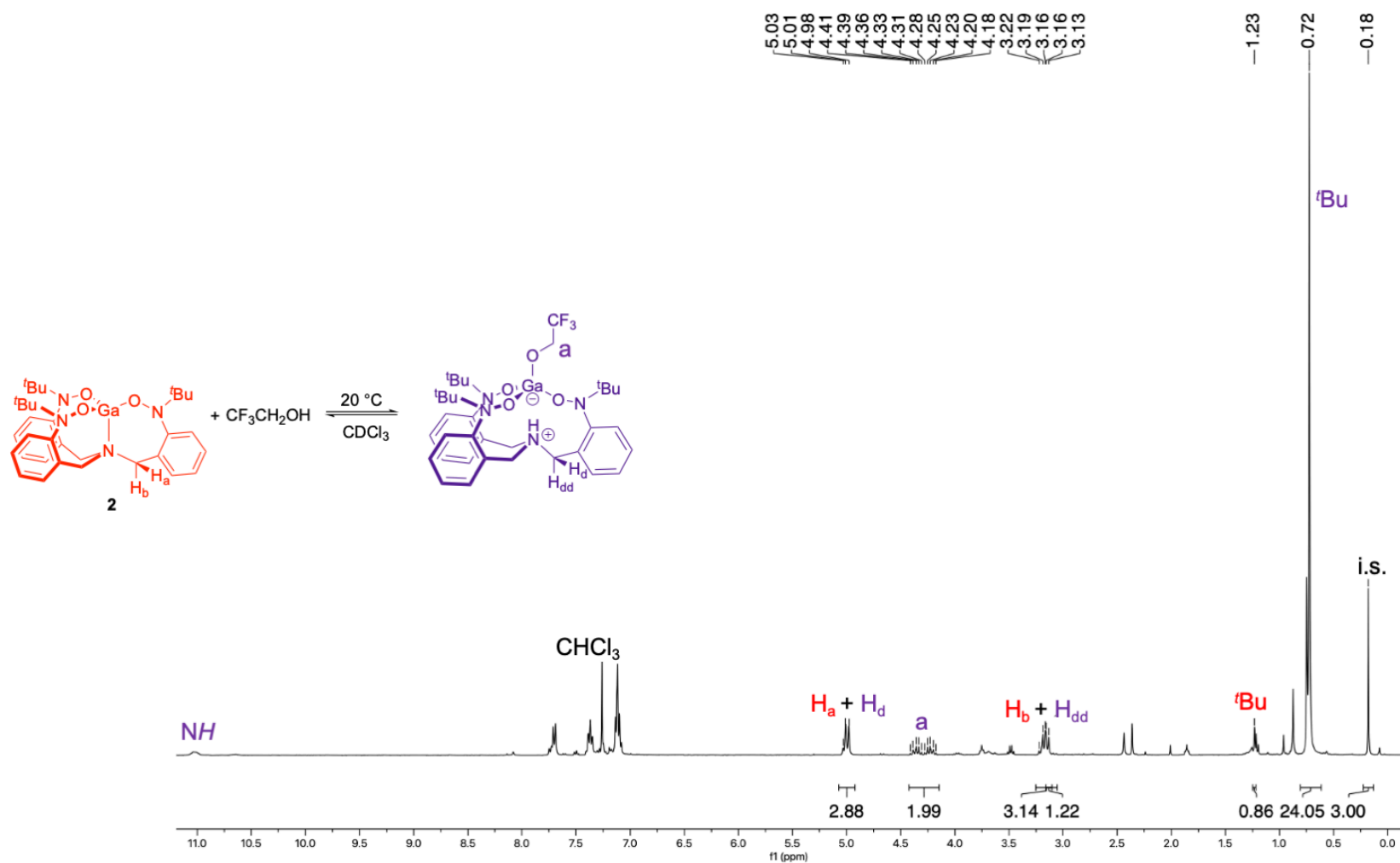


**Figure S28.**  $^1\text{H}$  NMR spectrum of a 1:1 mixture of **2**: $\text{CF}_3\text{CH}_2\text{OH}$ . Taken in  $\text{CDCl}_3$  and recorded after 24 hours of stirring at room temperature (Table 1, entry 7).



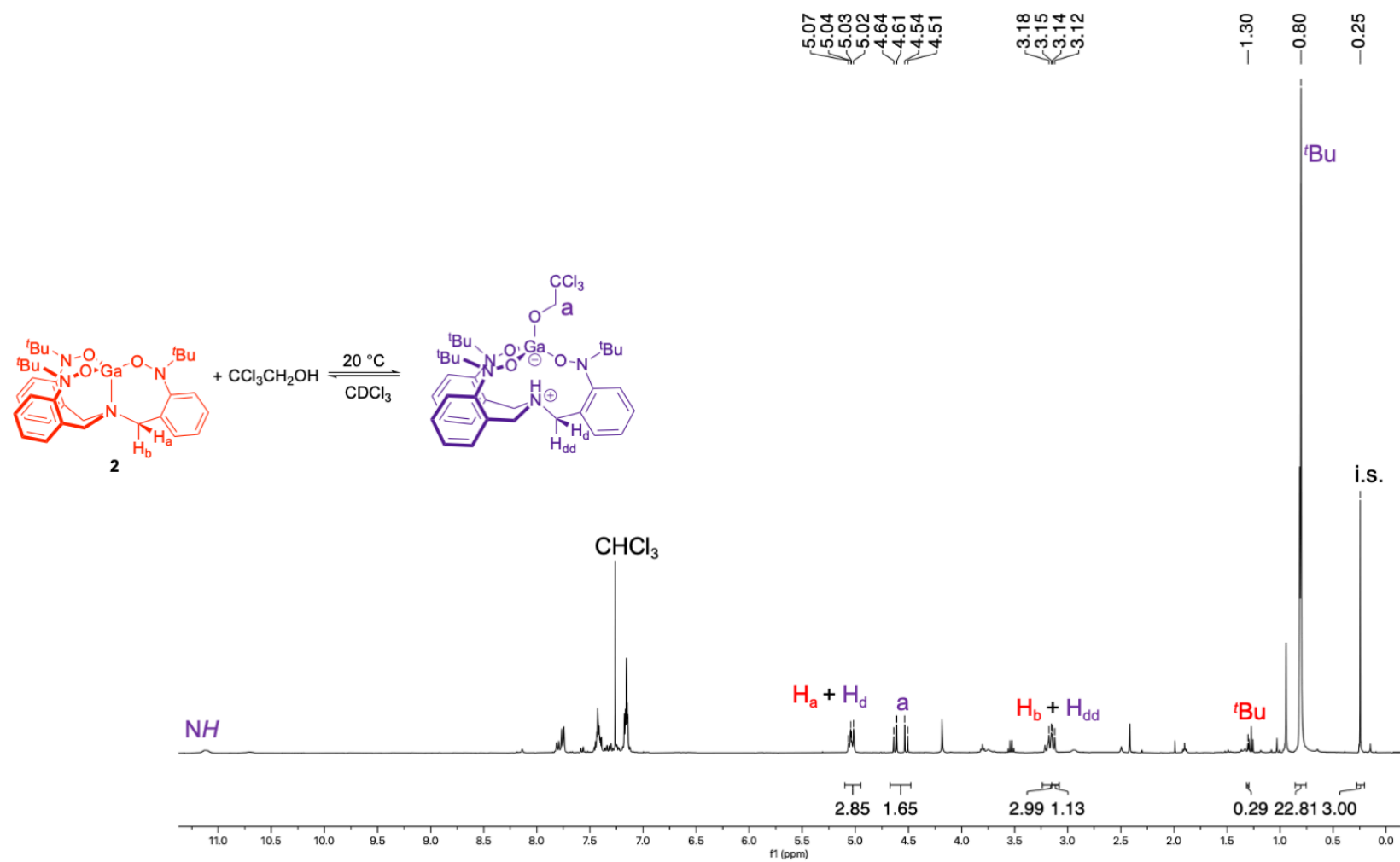


**Figure S29.**  $^1\text{H}$  NMR spectrum of a 1:1 mixture of **2**: $\text{CCl}_3\text{CH}_2\text{OH}$ . Taken in  $\text{CDCl}_3$  and recorded after 24 hours of stirring at room temperature (Table 1, entry 8).

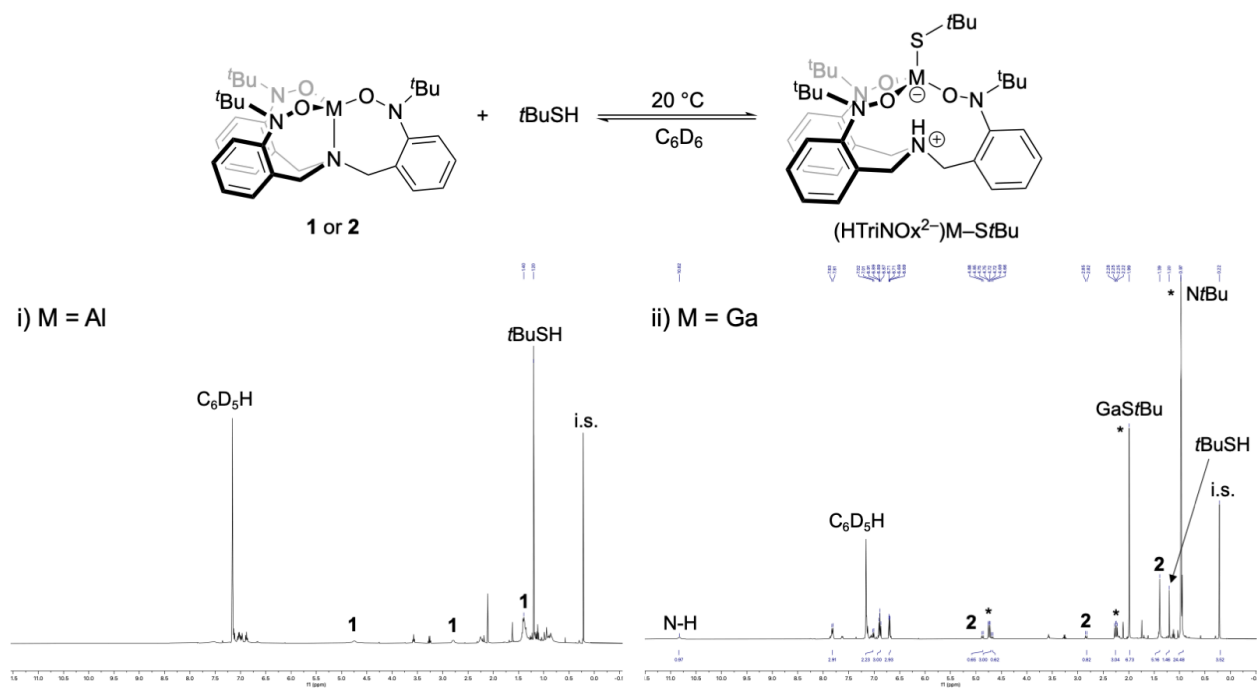


**Figure S30.**  $^1\text{H}$  NMR spectra of the reaction of *t*-BuSH with **1** (i) and **2** (ii) in  $\text{C}_6\text{D}_6$  recorded after 24 hours of stirring at room temperature. Resonances for the presumptive  $(\text{HTrINOx}^{2-})\text{Ga-S'tBu}$  product are labeled with an \*. i.s. = internal standard = hexamethylcyclotrisiloxane

**Protocol for kinetic analysis of the reactions of 1 and 2 with alcohols.** In the glovebox, 500  $\mu\text{L}$  of a 9 mM stock solution of **1** (or **2**) in  $\text{C}_6\text{D}_6$  was dispensed into an NMR tube along with 125  $\mu\text{L}$  of a 6 mM stock solution of hexamethylcyclotrisiloxane as an internal standard, also in  $\text{C}_6\text{D}_6$ . The NMR tube was sealed with a septa-lined cap, removed from the glovebox, and transported to the NMR spectrometer which has the temperature probe set to 20  $^\circ\text{C}$ . Once at the instrument, 125  $\mu\text{L}$  of a 36 mM stock solution of the specific alcohol in  $\text{C}_6\text{D}_6$  was added to the NMR tube via syringe through the septa, the tube was inverted once to start the experiment (time = 0), and the NMR sample was loaded into the NMR spectrometer. Single-scan  $^1\text{H}$  NMR spectra of the reaction were recorded at regular 2 min intervals and the concentration of the  $\text{H}(\text{TriNOx})^2\text{M-OR}$  complexes were determined by integration of the protons on the apical alkoxy ligands (-OR) against internal standard. For each experiment,  $[\mathbf{1}]_0$  (or  $[\mathbf{2}]_0$ ) =  $[\text{ROH}]_0$  = 6 mM; [i.s.] = 1 mM. The total reaction volume is 0.75 mL.

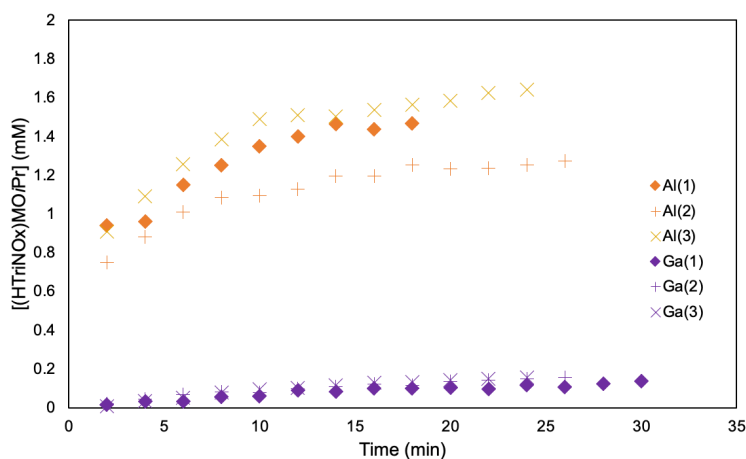


**Figure S31.** Plot showing the concentration of products over time for the reaction of **1** and **2** with *i*-PrOH in  $\text{C}_6\text{D}_6$  at 20  $^\circ\text{C}$ .

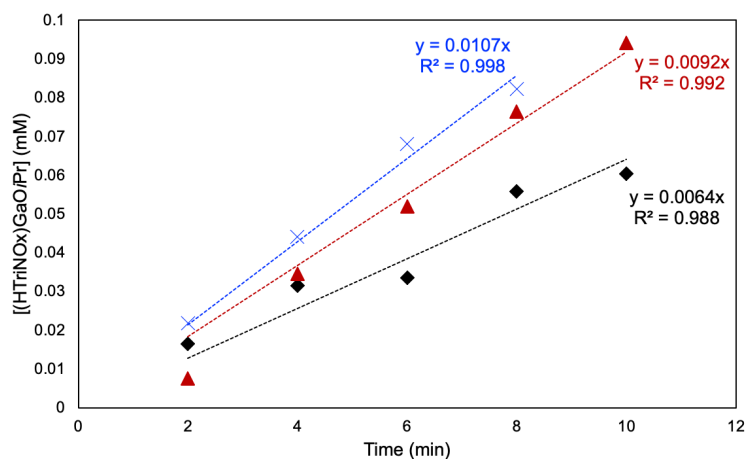


**Figure S32.** Initial rate data for the reaction of **2** with *i*-PrOH in  $\text{C}_6\text{D}_6$  at 20  $^\circ\text{C}$ . Replicate trials are represented by blue, black, and red lines.

**Procedure for the calculations to give the predicted- $pK_a$  of alcohols in DMSO.** All optimization and frequency calculations were performed with the Gaussian '16, Revision B.01 program using the G4 method<sup>1</sup> implementing a SCRF polarizable continuum solvent model of DMSO ( $\epsilon = 46.826$ ).

Predicted  $pK_a$  values were determined by calculating the Gibbs standard free energies for the alcohols and their corresponding alkoxide conjugate bases (Table S1). The difference of these energies for each alcohol/alkoxide pair represents the  $\Delta G^0$  of deprotonation ( $\Delta G^0_{\text{deprot}}$ ) for each alcohol (Table S2). The  $\Delta G^0_{\text{deprot}}$  values across the range of alcohols were normalized to 2,2,2-trifluoroethanol ( $\Delta G^0_{\text{deprot,ref}}$ ) and then converted to their corresponding calculated  $pK_a$  values via the following formula:

$$pK_a = -\log \left[ 10^{\frac{-\Delta G_{\text{deprot,ref}}}{C}} \right] \quad (\text{Eq. S3})$$

where C is equal to  $[1.9872 \text{ cal/K}\cdot\text{mol} * 298.15 \text{ K} * [\ln(10)/1000]]$ . These values represent the  $pK_a$  of the alcohols relative to 2,2,2-trifluoroethanol and although the absolute values hold no meaning, their relative values can be compared. To do so, we generated a calibration curve (Figure S38) between these calculated  $pK_a$  values and the  $pK_a$  values listed in the Bordwell literature for any alcohol with the latter value being available in DMSO. The line-of-best-fit equation was then used to determine the predicted  $pK_a$  values. Table S2 lists these predicted  $pK_a$  values for the range of alcohols studied along with the values from the Bordwell literature.<sup>2</sup>

---

<sup>1</sup> Curtiss, L. A.; Redfern, P. C.; Raghavachari, K. *J. Chem. Phys.* **2007**, *126*, 084108.

<sup>2</sup> Reich, H. Bordwell  $pK_a$  Table. <https://organicchemistrydata.org/hansreich/resources/pka/>

**Table S1.** Raw calculated Gibbs standard free energies at 298 K of alcohols and their corresponding alkoxides.

<b>alcohol (ROH)</b>	<b>Electronic energy + free energy correction of protonated form (hartrees)</b>	<b>Electronic energy + free energy correction of deprotonated form (hartrees)</b>
MeOH	-115.67961	-115.17672
EtOH	-154.96476	-154.46275
<i>t</i> BuOH	-233.53866	-233.03685
<i>i</i> PrOH	-194.25147	-193.75025
1-AdOH	-465.66954	-465.16899
BnOH	-346.60935	-346.11296
9-Me-FlOH	-615.64647	-615.15071
HC≡CCH <sub>2</sub> OH	-191.79935	-191.30800
CF <sub>3</sub> CH <sub>2</sub> OH	-452.67243	-452.18816
CCl <sub>3</sub> CH <sub>2</sub> OH	-1533.42630	-1532.94569
4-MeO-C <sub>6</sub> H <sub>4</sub> OH	-421.80596	-421.33244
PhOH	-307.33497	-306.86398
(CF <sub>3</sub> ) <sub>2</sub> CHOH	-789.65321	-789.18690

**Table S2.** Calculated standard Gibbs free energies of deprotonation ( $\Delta G_{\text{deprot}}$ ) in DMSO for alcohols and the manipulation of that data to give predicted  $pK_a$  values for alcohols.

alcohol (ROH)	$\Delta G_{\text{deprot}}^0$ (kcal/mol)	$\Delta G_{\text{deprot,ref}}^0$ <sup>a</sup> (kcal/mol)	Calculated $pK_a$ <sup>b</sup>	Predicted $pK_a$ <sup>c</sup>	Bordwell $pK_a$ <sup>d</sup>
MeOH	315.57	11.68	8.56	30.77	29
EtOH	315.02	11.13	8.16	30.43	29.8
<sup>t</sup> BuOH	314.90	11.01	8.07	30.36	32.2
<sup>i</sup> PrOH	314.52	10.63	7.79	30.12	30.25
1-AdOH	314.10	10.21	7.49	29.86	—
BnOH	311.49	7.60	5.57	28.26	—
9-Me-FIOH	311.09	7.21	5.28	28.01	—
HC≡CCH <sub>2</sub> OH	308.33	4.44	3.26	26.31	—
CF <sub>3</sub> CH <sub>2</sub> OH	303.89	0	0	23.58	23.5
CCl <sub>3</sub> CH <sub>2</sub> OH	301.58	-2.30	-1.69	22.16	—
4-MeO-C <sub>6</sub> H <sub>4</sub> OH	297.14	-6.75	-4.95	19.42	19.1
PhOH	295.55	-8.34	-6.11	18.44	18
(CF <sub>3</sub> ) <sub>2</sub> CHOH	292.61	-11.27	-8.26	16.64	17.9

a)  $\Delta G_{\text{deprot}}^0(\text{ROH}) - \Delta G_{\text{deprot}}^0(\text{CF}_3\text{CH}_2\text{OH})$ ; b) Relative to CF<sub>3</sub>CH<sub>2</sub>OH.; c) Determined using the line-of-best-fit in Figure S38; d) Values are quoted in DMSO and taken from Reich, H. Bordwell  $pK_a$  Table. <https://organicchemistrydata.org/hansreich/resources/pka/>.

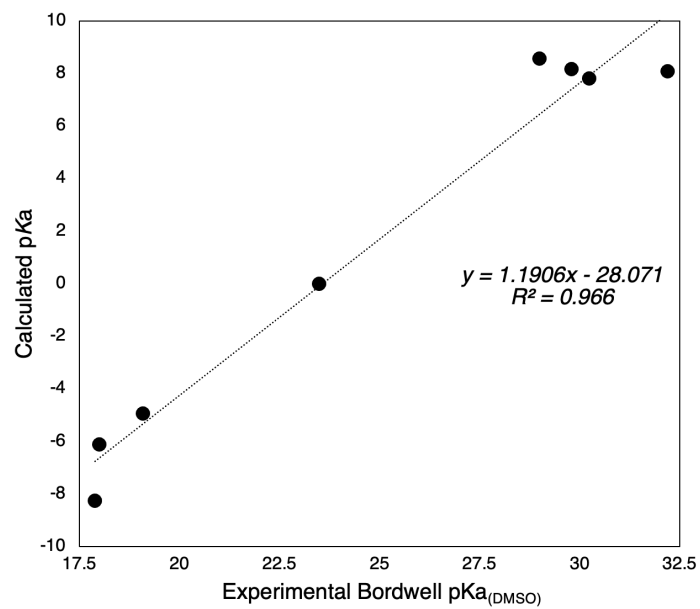


**Figure S33.** Correlation plot between the G4-calculated versus experimental determined  $pK_a$  values for alcohols.

**Procedure for the calculations to determine the A-values for the alcohol R groups.** All optimization and frequency calculations were performed with the Gaussian '16, Revision B.01 program using the G4 method.REF The geometries of both axial and equatorial conformers of the R-substituted cyclohexanes for each alcohol R group were optimized and the standard Gibbs free energy ( $\Delta G^0$ , in kcal/mol) values were calculated. The A-value for a given R substituent is a measurement of how much the equatorial conformer of the R-substituted cyclohexane is favored over the axial conformer. The A-values are thus obtained by subtracting  $\Delta G^0_{\text{equatorial}}$  from  $\Delta G^0_{\text{axial}}$ .

**Table S3.** Calculated standard Gibbs free energies at 298 K of the equatorial ( $\Delta G^0_{\text{equatorial}}$ ) and axial ( $\Delta G^0_{\text{axial}}$ ) conformers of R-substituted cyclohexanes and the calculated A-values for the R groups.



R Group	$\Delta G^0_{\text{equatorial}}$ (hartrees)	$\Delta G^0_{\text{axial}}$ (hartrees)	A-value (kcal/mol)
<i>t</i> -Bu	-392.880887	-392.871382	5.96
<i>i</i> -Pr	-353.597397	-353.593586	2.39
1-adamanyl	-625.040039	-625.035467	2.87
Me	-275.027013	-275.023177	2.41
Bn	-506.002444	-505.998587	2.42
9-MeFl	-775.083576	-775.083904	-0.21
HCCCH <sub>2</sub>	-351.157602	-351.153909	2.32
CF <sub>3</sub> CH <sub>2</sub>	-612.065504	-612.062007	2.19
CCl <sub>3</sub> CH <sub>2</sub>	-1693.113611	-1693.109934	2.31
4-OMe-C <sub>6</sub> H <sub>4</sub>	-581.207238	-581.200354	4.32
Ph	-466.714283	-466.707497	4.26



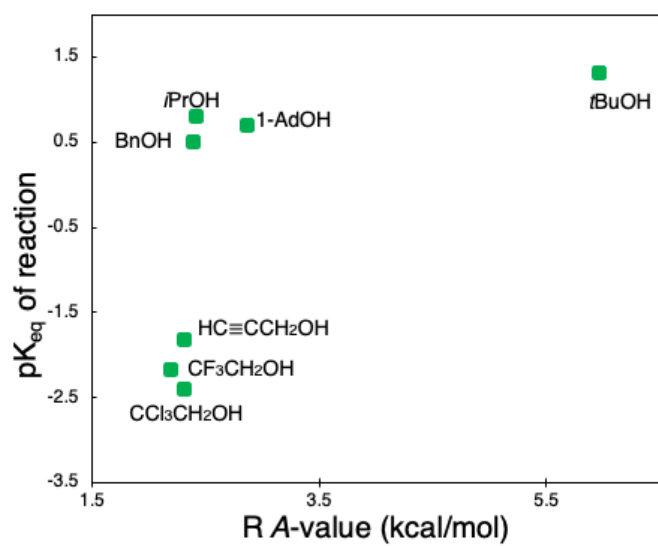


**Figure S34.** Plot of the  $pK_{eq}$  of the reaction of **2** with alcohol versus the A-value of the alcohol R group.